A STUDY OF MODELING FOR DYNAMIC STRESS SIMILITUDE

Thesis by

Richard Manning Hermes

In Partial Fulfillment of the Requirements

For the Degree of

Doctor of Philosophy

California Institute of Technology

Pasadena, California

1950

"Every man should marry. If he marries a good wife he will be very happy; if not, he will become a philosopher."

Socrates

This thesis is dedicated to my wife who has proven that the first antecedent does not preclude the second consequent.

ACKNOWLEDGMENTS

The author wishes to acknowledge with deep appreciation all who have helped to make this thesis possible. In particular he would express his sincere gratitude to Professor D. E. Hudson for his untiring assistance and guidance; to the Office of Naval Research for its financial support of this research at the University of Santa Clara; to the University of Santa Clara for providing laboratory facilities and equipment; to the California Institute of Technology for the use of laboratory equipment in those parts of the work which were carried out on that campus; and to Mary Bitgood for the excellent typography.

ABSTRACT

The prediction of stresses developed in structures subjected to dynamic loading constitutes a problem which is receiving increased attention on the part of engineers. The use of models for this prediction offers an economical and practical solution to this problem. In this paper the modeling parameters for vibrating beams are developed through an analysis in which the equations of motion are reduced to dimensionless form. The validity of these modeling parameters has been tested experimentally. These experiments are reported herein. It is further shown that this method of analysis can be extended to problems involving plates and frames.

TABLE OF CONTENTS

		Page
Abstract		
Introduction	....	1
Chapter		
I Analysis	....	6
II Experimentation	....	36
III Discussion of Results	....	59
IV Extension of the Theory	....	81
Bibliography	....	90
Appendices	....	91

INTRODUCTION

The study of engineering problems through the use of models is sound practice of long standing and is so widely used in the various branches of fluid mechanics as to need no further introduction.

Efforts have been made to attack problems in the mechanics of structures by models. Thus, the field of photoelasticity has been developed, as have the soap film analogy for torsional stress,[1] the electric potential analogy for stress concentration[2] and others[3] which are very useful in the study of static stresses. For the study of dynamic stresses, the few modeling methods which have been reported have had as their primary objective the determination through the use of a model of a structure its modes of vibration and their natural frequencies.[3] This information while of importance is not sufficient for the solution of many of the problems which arise in practice.

To realize the shortcomings of modeling methods which reveal only the modes of vibration of a structure and the frequencies of these modes, consider the following situation. For a simple cantilever beam the modes of vibration and their frequencies can easily be calculated. Yet from this knowledge, it is not possible to calculate the stresses developed in the beam if its root is subjected to a sudden acceleration. An approximate solution for these stresses was offered by

---

(1) Numbers in ( ) refer to the Bibliography.

Sezawa[4], and the approximation has been improved by Mindlin[5]. The fact remains that an experimental investigation of these stresses is essential for their accurate determination. If the structure is large, the study of a model designed for dynamic stress similitude becomes imperative.

The question immediately arises as to what constitutes modeling for dynamic stress similitude. The answer may be given broadly: "A structure is correctly modeled for dynamic stress similitude if from the measured stresses in the model the stresses in the structure under given dynamic load can be predicted within the limits of engineering accuracy."

Various portions of this statement require further consideration:

There is nothing in this criterion which requires geometric similarity. While there is no objection to making the model geometrically similar to the prototype if this is easily accomplished, it would be desirable if possible to have greater freedom in the construction of the model than is usually allowed by a requirement of geometric similarity. The omission of small details or the choice of a shape which will easily carry strain gages are examples. Likewise a change of materials, e.g. using brass to model a steel prototype, will frequently lead to easier fabrication.

The stresses developed in prototype and model need not be the same; the ability to calculate strains in the prototype is all that is sought. It appears desirable because of the reliability and availability of the electric resistance strain gage to base the modeling on similitude of strains. By means of Young's modulus, stress similitude is thus attained. In fact, throughout this paper stress similitude and strain similitude are taken as logically equivalent, i.e. either condition implies the other.

In addition to the conditions which must be satisfied by a model for dynamic stress similitude, there will be conditions which must be satisfied by the load to which the model is subjected.

Finally, careful consideration must be given to the limitations imposed by the desire that the stresses predicted be within the limits of engineering accuracy. The concept of engineering accuracy is admittedly nebulous. Under certain circumstances a disagreement between predicted and observed results of, say, 3 percent is inacceptable while under other circumstances errors of the order of magnitude of 50 percent or more are considered not too large. In spite of this wide range, it seems advantageous to establish limits of accuracy to serve primarily as a criterion by which the success of the modeling method to be developed can be judged. To this end we consider the ordinary procedure of stress analysis. For as common and carefully controlled a material as steel, ASME Specification S-1, for example, the easily measured property of ultimate strength is always given with a range of 10,000 psi, namely, the ultimate strength if specified as 55,000 psi to 65,000 psi. Moreover, ASTM standards do not require a testing machine to have accuracy greater than 5 percent. These two facts yield a range of 16,000 psi in the ultimate strength of this material. This is an accuracy of 13.3 percent of the mean value of this property. It appears, then, that a structure can be considered to have been satisfactorily modeled if the difference between the stresses as predicted from the model and the stresses developed in the prototype is less than 10 percent to 12 percent of the latter.

It is the object of this paper to establish the parameters for the modeling of dynamic stresses. The approach used is as follows: In Chapter I the modeling parameters are revealed through an analysis of the equation of motion of a prismatical bar. The results of this analysis are then verified experimentally. This experimentation is reported in Chapter II. A discussion of results is undertaken in Chapter III. The method of analysis is then extended to other vibrating systems in Chapter IV. In the Appendices are assembled items of interest which developed in the course of this study but which are somewhat irrelevant to Chapters I-IV. These consist of Appendix I: The eigen-functions, frequency equation, and the first five natural frequencies, all in dimensionless form for the six types of beams; Appendix II: Demonstration of the normality of the dimensionless eigen-functions; Appendix III: Speed of sound for various materials; Appendix IV: Expansion of the Statical Deflection Curve of a Cantilever

Beam with concentrated load at the free end in a series of eigen-functions; Appendix V: The frequency equation for a frame.

CHAPTER I

It has been pointed out many times that, although the dynamic stresses depend on the amount of damping present, an analysis based on the assumption of no damping is frequently of considerable value.[8] Accordingly, the following analysis falls into two parts: In Part I an analysis is developed neglecting damping; in Part II the analysis includes the effect of internal damping. The method of attack is the same in both parts of the analysis. It consists of reducing the equations of motions to dimensionless form through the introduction of properly selected dimensionless variables. The choice of dimensionless variables for lengths offers no problem; each length variable is referred to some characteristic length of the structure. It is also necessary to introduce a dimensionless time. This is accomplished by referring time variables to the time required for a small disturbance (i.e. an elastic wave) to travel the characteristic length.

FREE VIBRATIONS WITHOUT DAMPING:

Consider a straight bar of length L and of uniform cross section and density, free to vibrate in one of its principal planes of flexure. Let this plane coincide with an x-y plane the origin of coordinates being taken at the left end of the bar, the x-axis coinciding with the equilibrium position of its centroidal axis. The equation of motion is (15)

$$EI \frac{\partial^4 y}{\partial x^4} = -\frac{\gamma A}{g} \frac{\partial^2 y}{\partial t^2} \tag{1}$$

with the boundary conditions

$$
\left.
\begin{array}{l}
\underline{\text{Hinged-hinged beam:}} \\
\quad y(0,t) = y''(0,t) = y(L,t) = y''(L,t) = 0; \\[1em]
\underline{\text{Free-free beam:}} \\
\quad y''(0,t) = y'''(0,t) = y''(L,t) = y'''(L,t) = 0; \\[1em]
\underline{\text{Fixed-fixed beam:}} \\
\quad y(0,t) = y'(0,t) = y(L,t) = y'(L,t) = 0; \\[1em]
\underline{\text{Free-hinged beam:}} \\
\quad y'''(0,t) = y''(0,t) = y(L,t) = y'''(L,t) = 0; \\[1em]
\underline{\text{Fixed-hinged beam:}} \\
\quad y(0,t) = y'(0,t) = y(L,t) = y''(L,t) = 0; \\[1em]
\underline{\text{Fixed-free beam:}} \\
\quad y(0,t) = y'(0,t) = y''(L,t) = y'''(L,t) = 0;
\end{array}
\right\} \qquad (A)
$$

where E = Young's Modulus

γ = specific weight of the material

A = cross-sectional area of the bar

I = moment of inertia of the section about neutral axis

g = acceleration due to gravity

y = displacement of the neutral axis

x = distance from left-end of bar

t = time

It should be recalled that a physical variable, for example a length, x, is the product of a pure numeric and a scale constant. We write x = 3 feet or x = 3 inches as the case might be. With more generality we write $x = L\xi$ where ξ is a pure numeric and L is the scale constant. Algebraic processes deal only with the pure numeric, and the physical process is completely described mathematically by equations relating the ξ-type variables, the L-type entering only to fix the scale. Therefore two different structures will be undergoing the same physical process if their ξ-type variables satisfy the same equations. With this in mind we proceed to remove the scale constants from Eq. (1).

Define

a = velocity of propagation of small disturbances in the material

k = radius of gyration of the section about the neutral axis

$x = L\xi$

$y = L\eta$

$k = L\kappa$

$t = \frac{L}{a}\tau$

$A = L^2\alpha$

By differentiation, we find that

$$\frac{\partial^n y}{\partial x^n} = L^{-n+1}\frac{\partial^n \eta}{\partial \xi^n} \qquad (n = 1, 2, \cdots)$$

and

$$\frac{\partial^n y}{\partial t^n} = a^n L^{-n+1}\frac{\partial^n \eta}{\partial \tau^n} \qquad (n = 1, 2, \cdots) \qquad \text{(A)}$$

Substitution of the foregoing expressions in Eq. (1) and Cond. (A) yields

(2) $$k^2 \frac{\partial^4 \eta}{\partial \xi^4} = - \frac{\partial^2 \eta}{\partial \tau^2}$$

and

$$\left.\begin{array}{l} \eta(0,\tau) = \eta''(0,\tau) = \eta(1,\tau) = \eta''(L,\tau) = 0 \\ - \; - \; - \; - \; - \; - \; - \; - \\ \eta(0,\tau) = \eta'(0,\tau) = \eta''(1,\tau) = \eta'''(1,\tau) = 0 \end{array}\right\} \quad (B)$$

where all the expressions are dimensionless.

Equation (2) is solved in the usual way by assuming that a solution exists in the form

(3) $$\eta = \Xi(\xi)\, T(\tau)$$

which leads to

(4) $$\Xi(\xi) = c_1 \sin p\xi + c_2 \cos p\xi + c_3 \sinh p\xi + c_4 \cosh p\xi$$

(5) $$T(\tau) = A \cos \omega\tau + B \sin \omega\tau$$

where

(6) $$p^2 = \frac{\omega}{k}$$

The satisfaction of the boundary conditions by Eq. (4) yields the values of c_1, c_2, c_3, and c_4, and leads to the frequency equation together with an infinite sequence of values for p. This done, the solution of Eq. (2) can be shown in the form

(7) $$\eta = \sum_{i=1}^{\infty} c_i\, \Xi_i(\xi)\, T_i(\tau)$$

where

(8) $$\Xi_i(\xi) = \sin p_i\xi + \alpha_1 \cos p_i\xi + \alpha_2 \sinh p_i\xi + \alpha_3 \cosh p_i\xi$$

and

(9) $$T_i(\tau) = \cos \omega_i\tau + D_i \sin \omega_i\tau$$

It is to be noted that the $\Xi_i(\xi)$ constitute, except for the hinged-hinged beam, a normalized orthogonal set.* To normalize the exceptional case it is only necessary to replace c_i by $c_i\sqrt{2}$ in Eq. (7).

To evaluate Eq. (7) for the initial conditions, let it be assumed that at time t = 0, the beam is given a configuration y = f(x,0) and is released with a velocity $\frac{\partial y}{\partial t} = v(x,0)$. These conditions are rendered dimensionless by writing

$$\left.\begin{aligned} \eta &= \frac{1}{L} f(L\xi,\ 0) = F(\xi, 0) \\ \text{and} \qquad \frac{\partial \eta}{\partial \tau} &= \frac{1}{a} v(L\xi, 0) = G(\xi, 0) \end{aligned}\right\} \qquad \text{(C)}$$

The coefficients c_i and D_i are then evaluated in the usual manner, keeping in mind the normality of the functions $\Xi_i(\xi)$. Thus, for example, the expression for c_i is

(10) $$c_i = \int_0^1 F(\xi;0)\,\Xi_i(\xi)\,d\xi$$

A consideration of Eq. (2) and Cond. (C) reveals that for a prototype and model to have the same dimensionless equation of motion, namely Eq. (7), the following conditions will have to be satisfied (p refers to prototype, m to model):

*See Appendix II

$$\left.\begin{aligned} \frac{K_p}{K_m} &= \frac{L_p}{L_m} \\ \frac{f_p(x,0)}{f_m(x,0)} &= \frac{L_p}{L_m} \\ \frac{V_p(x,0)}{V_m(x,0)} &= \frac{a_p}{a_m} \end{aligned}\right\} \quad \text{(D)}$$

and the method of support must be the same for each beam.

From the known formula $s = E\, d_0 \left.\frac{\partial^2 y}{\partial x^2}\right|_{x=x_0}$, the stress in the beam at the point (x_0, d_0), where d_0 is the distance of the point under consideration from the neutral axis, can be expressed dimensionlessly as

$$\frac{s}{E} = d_0 \left.\frac{\partial^2 y}{\partial x^2}\right|_{x=x_0}$$

Since we can write d_0 dimensionlessly as $\delta_0 = \frac{d_0}{L}$ and $\frac{\partial^2 \eta}{\partial \xi^2} = L \frac{\partial^2 y}{\partial x^2}$, we find

(11) $$\frac{s}{E} = \delta_0 \left.\frac{\partial^2 \eta}{\partial \xi^2}\right|_{\xi=\xi_0}$$

Whence it follows immediately that for prototype and model satisfying Conditions (C) and (D)

(12) $$\frac{s_p}{E_p} = \frac{s_m}{E_m}$$

i.e., that

(12a) $$\epsilon_p = \epsilon_m$$

where ϵ is unit strain.

FORCED VIBRATIONS WITHOUT DAMPING:

In order to deal with forced vibrations, we take as generalized coordinates $q_i = c_i T_i(\tau)$. Then Lagrange's equations of motion can be put into dimensionless form. In ordinary form, these equations are

(13) $$\frac{d}{dt}\left(\frac{\partial T}{\partial \dot{q}_i}\right) - \frac{\partial T}{\partial q_i} + \frac{\partial V}{\partial q_i} = Q_i \qquad (i = 1, 2, \cdots)$$

where

$$T = \frac{\gamma A}{2g}\int_0^L \dot{y}^2 dy \qquad \text{and} \qquad V = \frac{EI}{2}\int_0^L \left(\frac{\partial^2 y}{\partial x^2}\right)^2 dx$$

In these equations we make the substitutions (a) and also the following

$$T = \frac{\gamma A}{2g}\int_0^L \dot{y}^2 dy = \frac{\gamma A}{2g} a^2 L \sum_{i=1}^{\infty}\left(\frac{\partial q_i}{\partial \tau}\right)^2 \qquad *$$

$$V = \frac{EI}{2}\int_0^L \left(\frac{\partial^2 y}{\partial x^2}\right)^2 dx = \frac{EI}{2L}\sum_{i=1}^{\infty} q_i \frac{\omega_i^2}{k^2}$$

and

$$\frac{d}{dt}\left(\frac{\partial T}{\partial \dot{q}_i}\right) = \frac{d}{d\tau}\left(\frac{\partial T}{\partial\left(\frac{\partial q_i}{\partial \tau}\right)}\right).$$

This yields as the Lagrangian Equation of Motion in dimensionless form:

(14) $$\frac{d^2 q_i}{d\tau^2} + \omega^2 q_i = \frac{g}{\gamma A a^2 L} Q_i \qquad (i = 1, 2, \cdots)$$

The conditions which must be satisfied in order to model a beam subjected to a forcing function can be determined from a consideration of the right-hand side of Eq. (14). For example, suppose a force $P = P_\circ f(t)$ acts on the

---

*The $\oint$ does not appear because of the normality of the Ξ_i functions.

beam at the point $x = b$. Now Q_i is the work done by this force under the variation q_i. Since $\eta = \frac{y}{L} = \sum_{i=1}^{\infty} \Xi_i(\xi) q_i$ and $\delta y_i = L\, \Xi_i(\xi)\, \delta q_i$

it follows that

$$Q = L P \cdot f(t)\, \Xi_i\left(\frac{b}{L}\right), \quad (i = 1, 2, \cdots\cdots)$$

Moreover, if we write $A = L^2\alpha$, Eq. (14) assumes the form

$$(15) \qquad \frac{d^2 q_i}{d\tau^2} + \omega_i^2 q_i = \frac{Pg}{\gamma \alpha a^2 L^2}\, \Xi_i\left(\frac{b}{L}\right) f\left(\frac{L\tau}{a}\right), \quad (i = 1, 2, \cdots\cdots)$$

To model satisfactorily a beam subjected to a concentrated forcing function, we must satisfy not only Conditions (D) but also

$$\frac{P_p g}{\gamma_p \alpha_p a_p^2 L_p^2}\, f\left(\frac{L_p \tau}{a_p}\right) = \frac{P_m g}{\gamma_m \alpha_m a_m^2 L_m^2}\, f\left(\frac{L_m \tau}{a_m}\right) \qquad (E)$$

The generality inherent in Cond. (E) is not often necessary in a modeling investigation. More frequently will it be desired to maintain similarity. In this event $\alpha_p = \alpha_m$. Furthermore, if the forcing function be periodic, say $P_p\, f_p(t) = P_p \sin \Omega_p t$, then Cond. (E) becomes

$$\frac{P_p}{\gamma_p a_p^2 L_p^2} \sin \frac{\Omega_p L_p \tau}{a_p} = \frac{P_m}{\gamma_m a_m^2 L_m^2} \sin \frac{\Omega_m L_m \tau}{a_m}$$

For this to be an identity, it is sufficient that

$$\left.\begin{aligned} \frac{\Omega_p L_p}{a_p} &= \frac{\Omega_m L_m}{a_m} \\ \text{and} \qquad \frac{P_p}{\gamma_p a_p^2 L_p^2} &= \frac{P_m}{\gamma_m a_m^2 L_m^2} \end{aligned}\right\} \qquad (E_1)$$

THE FREE VIBRATION OF A BEAM WHOSE BOUNDARY CONDITIONS ARE FUNCTIONS OF TIME:

When using small models, the application of a forcing function to the model is frequently difficult. This difficulty can be avoided by subjecting the beam to boundary conditions which are functions of time. The foregoing method of analysis can be satisfactorily used for this type of vibration also. By way of example, consider a prismatical cantilever beam having one of its principal planes of flexure coinciding with the x-y plane and free to vibrate in this plane. Let its root move along the y-axis with the velocity v, and let its centroidal axis remain parallel with the x-axis. At time $t = 0$ let the axis of the beam coincide with the x-axis and let its root be given an acceleration $f(t)$. The mathematical complications resulting from the initial velocity v can be obviated by referring the subsequent motion to axes with origin at the root and parallel with the x-y axes. To do this, we write $y = y_0 + w$, where y is the displacement of any point of the beam referred to the x-y axes, y_0 is the displacement of the beam referred to the x-y axes, and w is the displacement of any point of the beam referred to the axes with origin at the root. With this substitution, Eq. (1) becomes

$$(16) \qquad \frac{EIg}{\gamma A} \frac{\partial^4 w}{\partial x^4} + \frac{\partial^2 w}{\partial t^2} = - \frac{\partial^2 y_0}{\partial t^2}$$

The appropriate boundary and initial conditions on w are

a) $w(0,t) = 0$, d) $w''(L,t) = 0$,

b) $\dot{w}(0,t) = 0$, e) $w(x,0) = 0$,

c) $w'(L,t) = 0$, f) $\dot{w}(x,0) = 0$,

while the conditions on y_0 are

g) $\frac{\partial^2 y_0}{\partial t^2} = 0$ if $t \leq 0$,

h) $\frac{\partial^2 y_0}{\partial t^2} = f(t)$ if $t > 0$.

Using the definitions on page 4 and $w = L\omega$, Eq. (16) and its boundary and initial conditions can be put into dimensionless form:

$$\kappa^2 \frac{\partial^4 \omega}{\partial \xi^4} + \frac{\partial^2 \omega}{\partial \tau^2} = -\frac{\partial^2 \eta_0}{\partial \tau^2} \tag{17}$$

and

$$\left.\begin{array}{ll} \omega(0,\tau) = 0 & \frac{\partial^3}{\partial \xi^3}\omega(0,\tau) = 0 \\ \frac{\partial}{\partial \xi}\omega(0,\tau) = 0 & \omega(\xi,0) = 0 \\ \frac{\partial^2}{\partial \xi^2}\omega(1,\tau) = 0 & \frac{\partial}{\partial \tau}\omega(\xi,0) = 0 \\ \multicolumn{2}{c}{\frac{\partial^2 \eta_0}{\partial \tau^2} = 0 \quad \text{if} \quad \tau \leq 0} \\ \multicolumn{2}{c}{\frac{\partial^2 \eta_0}{\partial \tau^2} = \frac{L}{a^2} f\left(\frac{L\tau}{a}\right) \quad \text{if} \quad \tau > 0} \end{array}\right\} \quad (F)$$

In order to model dynamically for stress similitude, it is only necessary that Eq. (17) and Condition (F) be satisfied for both prototype and model.

As an immediate application of Condition (F) consider the case wherein f(t) is defined by

$$\left.\begin{aligned} f(t) &= 0 && \text{if} \quad t \leq 0 \\ f(t) &= b \sin \omega t && \text{if} \quad 0 \leq t \leq \frac{\pi}{\omega} \\ f(t) &= 0 && \text{if} \quad \frac{\pi}{\omega} \leq t \end{aligned}\right\} \qquad (18)$$

Then, writing these conditions in dimensionless form, we find

$$\left.\begin{aligned} \frac{\partial^2 \eta_0}{\partial \tau^2} &= 0 && \text{if} \quad \tau \leq 0 \\ \frac{\partial^2 \eta_0}{\partial \tau^2} &= \frac{Lb}{a^2} \sin \frac{\omega L \tau}{a} && \text{if} \quad 0 \leq \tau \leq \frac{\pi a}{\omega L} \\ \text{and} \quad \frac{\partial^2 \eta_0}{\partial \tau^2} &= 0 && \text{if} \quad \frac{\pi a}{\omega L} \leq \tau \end{aligned}\right\} \qquad (18')$$

From Condition (18') it follows that modeling will be correct if

$$\left.\begin{aligned} \left(\frac{Lb}{a^2}\right)_{\text{model}} &= \left(\frac{Lb}{a^2}\right)_{\text{prototype}} \\ \text{and} \quad \left(\frac{L\omega}{a}\right)_{\text{model}} &= \left(\frac{L\omega}{a}\right)_{\text{prototype}} \end{aligned}\right\} \qquad (F')$$

Returning to Eq. (1) and making the substitution $y = y_0 + w$ yields

$$(1') \qquad EI \frac{\partial^4 w}{\partial x^4} + \frac{\gamma A}{g} \frac{\partial^2 w}{\partial t^2} = - \frac{\gamma A}{g} \frac{\partial^2 y_0}{\partial t^2}$$

Eq. (1') is precisely the same as that for a cantilever beam with a uniformly distributed transverse load U(t) where

(19) $$U(t) = -\frac{\gamma A}{g}\frac{\partial^2 y_0}{\partial t^2}$$

To find the dimensionless expression involving the load U(t) (whose units, incidentally, are F/L), we shall multiply both sides of Eq. (19) by $-g/\gamma A$ and replace $\frac{\partial^2 y_0}{\partial t^2}$ by $\frac{a^2}{L}\frac{\partial^2 \eta_0}{\partial \tau^2}$. Thus

(20) $$\frac{\partial^2 \eta_0}{\partial \tau^2} = -\frac{g}{\gamma A}\frac{L}{a^2}U(t)$$

Furthermore, if we assume geometric similarity, then $A = L^2\alpha$ and Eq. (20) becomes

$$\frac{\partial^2 \eta_0}{\partial \tau^2} = -\frac{g\,U(t)}{\gamma \alpha L a^2}$$

Finally, if we put U(t) in the form

$$U(t) = \frac{P}{L}f(t)$$

where P is maximum total load on the beam, we reach

(21) $$\frac{\partial^2 \eta_0}{\partial \tau^2} = -\frac{g\,P f(t)}{\gamma \alpha L^2 a^2}$$

To model a uniformly loaded beam, the conditions to be satisfied are

$$\left(\frac{P f(\frac{L\tau}{a})}{\gamma L^2 a^2}\right)_{\text{model}} = \left(\frac{P f(\frac{L\tau}{a})}{\gamma L^2 a^2}\right)_{\text{prototype}} \qquad \text{(G)}$$

and the beams must be geometrically similar. It is to be observed that these conditions are precisely those for a beam with a concentrated load which were obtained by a different method.

As has already been stated, it is possible to use a model whose boundary conditions are functions of time instead of applying a forcing function to the model. The conditions which must be satisfied for such modeling can now be investigated.

Let the forcing function be a uniformly distributed load varying sinusoidally with time. Thus,

$$U(t) = \frac{P}{L} \sin p_0 t$$

As we have just seen, P must satisfy Condition (G), while

$$\left(\sin \frac{p_0 L \tau}{a}\right)_{\text{model}} = \left(\sin \frac{p_0 L \tau}{a}\right)_{\text{prototype}}$$

i.e. $$\left(\frac{p_0 L}{a}\right)_{\text{model}} = \left(\frac{p_0 L}{a}\right)_{\text{prototype}}$$

But this is precisely the condition for modeling under sinusoidal acceleration of the root. If b is the maximum acceleration, then by Eqs. (21) and (18') b must be so chosen that $$-\frac{g P \sin \frac{p_0 L \tau}{a}}{\gamma a^2 L^2 \alpha} = \frac{Lb}{a^2} \sin \frac{\omega L \tau}{a}$$

that is, so that if we select $\omega = p_0$

$$b_p = -\frac{g P_p}{\gamma_p \alpha L_p^3} \tag{22}$$

where the subscript p refers to the prototype. If Condition (G) is satisfied, then, with subscript m referring to model

$$\frac{P_m}{\gamma_m L_m^2 a_m^2} = \frac{P_p}{\gamma_p L_p^2 a_p^2}$$

whence $$b_p = -\frac{g P_m}{\gamma_m \alpha L_m^3} \cdot \frac{a_p^2 L_m}{a_m^2 L_p}$$

or $$\frac{b_p L_p}{a_p^2} = \frac{b_m L_m}{a_m^2}$$

which is precisely Condition (F'). If, therefore, b is chosen so that Eq. (22) is satisfied, and if geometrical similarity is maintained, the observance of Condition (F') will insure satisfactory modeling of the action of the beam under the forcing function

$$\frac{P}{L} \sin p_0(t)$$

A case of especial interest occurs when the time duration of the function f(t) is very small. Thus, in Fig. (1)

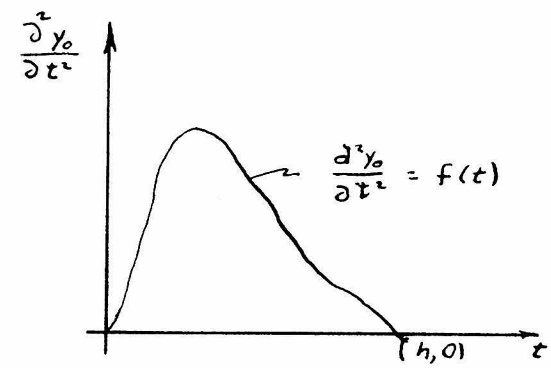

Fig. 1

let $h \ll 1$. Suppose moreover that

$$\int_0^h f(t)\,dt = A \tag{23}$$

The Laplace transform proves useful in evaluating the effects of such an acceleration on the system.

Substituting $t = \frac{L\tau}{a}$ and $f(t) = \frac{\partial^2 y_o}{\partial t^2} = \frac{a^2}{L}\frac{\partial^2 \eta_o}{\partial \tau^2}$ we find

$$\int_0^{\frac{ah}{L}} \frac{\partial^2 \eta_o}{\partial \tau^2}\, d\tau = \frac{A}{a} \tag{24}$$

Now the Laplace transform of f(t) is p A if h is very small. Whence the Laplace transform of the right-hand side of Eq. (17) for accelerations of very small duration is p A/a. Writing the Laplace transform of each term of Eq. (17), yields, if $\omega \supset \bar{\omega}$

$$k^2 \frac{\partial^4 \bar{\omega}}{\partial \xi^4} + p^2 \bar{\omega} = \frac{A}{a} p \tag{25}$$

as the transformed equation of motion to be solved with the boundary conditions

a') $\bar{\omega}(0) = 0$ c') $\bar{\omega}''(0) = 0$

b') $\bar{\omega}'(0) = 0$ d') $\bar{\omega}'''(0) = 0$

We conclude, then, that a prototype will be satisfactorily modeled if

$$\left.\begin{aligned} \left(\frac{K}{L}\right)_{model} &= \left(\frac{K}{L}\right)_{prototype} \\ \left(\frac{1}{a}\int_0^h f(t)\,dt\right)_{model} &= \left(\frac{1}{a}\int_0^h f(t)\,dt\right)_{prototype} \end{aligned}\right\} \quad \text{(H)}$$

and the duration of the acceleration is very short.* The

* h is small if $\int_0^h e^{-pt} f(t)\,dt \cong \int_0^h f(t)\,dt$

significance of this conclusion lies in the fact that if the duration of an impulse is short in comparison with the natural period of the structure, the same impulse should be applied to prototype and model.

MODELING BEAMS WITH INTERNAL DAMPING:

The literature on internal damping is extensive and, to a large extent, contradictory.[6] In this investigation interest lies in relatively high stresses - those lying in the range of engineering stresses. As a result the pertinent facts which appear to be reasonably established are:

1. Damping capacity was defined by Föppl as the energy dissipated per unit volume per cycle and specific damping capacity as the ratio of the energy dissipated per unit volume of material per cycle to the maximum strain energy per unit volume of material.[7] Thus in Fig. (2) which shows

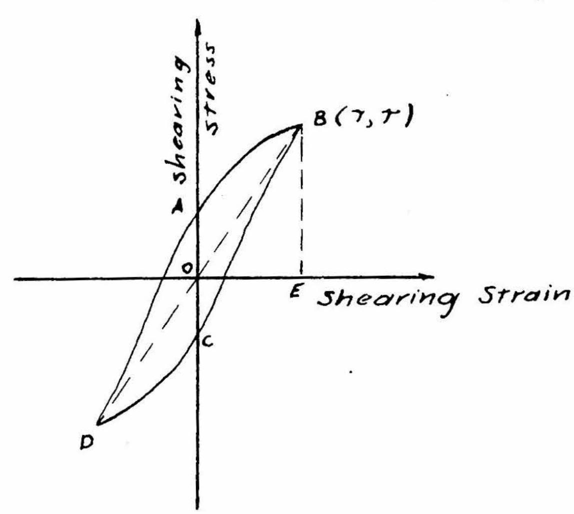

Fig. 2

the ordinary hysteresis loop, the damping capacity φ is the area of the loop ABCD while the specific damping capacity is the ratio of the area of the loop ABCD to the area of the triangle OBE. These quantities appear to be displacing others that had been previously used. The damping capacity of a material depends on the maximum shear stress τ, as well as on several other variables. However, an analysis can be carried out in terms of normal stress instead of shear stress because if we write

$$\phi = \phi(\tau)$$

it has been shown (5), (6) that

$$\phi = \phi(k\sigma)$$

where σ is the maximum normal stress.

2. The damping capacity φ depends on the history of the specimen. As a given specimen is subjected to repeated cycles of stress, the area of the hysteresis loop decreases. If the maximum stress is below the endurance limit, the damping capacity will become stabilized after approximately one million of stress reversals. If the maximum stress is above the endurance limit, the area of the damping capacity, after having decreased as in the previous case, increases markedly shortly before fatigue failure occurs.[8]

3. Kimball showed[9] that damping capacity is independent of frequency.* From this it is concluded that internal

*But see(10) who report that at higher temperatures (of the order of 700° F) damping capacity varies with frequency.

damping is not viscous; i.e. that the energy dissipated by internal damping is not due to the existence of a force which is proportional to velocity. Rather, the concept of internal damping is one of energy absorbed per cycle of vibration by virtue of the noncoincidence of the upward and downward branch of the load-deflection curve. Consequently, no damping force should appear in the equations of motion.[8] To overcome this difficulty, Jacobsen[11] has proposed a method of introducing the effect of internal damping into the equations of motion through the use of a coefficient of equivalent viscous damping. This method has been further developed by Mykelstad[12].

4. In the range of stress encountered in engineering practice, damping capacity appears to depend only on the maximum stress. It is common practice to write the energy dissipated, ΔW, as

$$\Delta W = c\tau^{n}$$

where c and n are constants to be determined by experiment. Various values of n have been offered: Mykelstad[12] states that n = 2.3 for steel. Robertson and Yorgiadis [14] give many curves of ΔW vs. τ_{max} for all of which n is 3. Kimball [13] offers the values of 2 or 3 for n. A dimensional analysis which is carried out below reveals that if we assume that ΔW is a function of stress and strain only, then W can be displayed in the form

$$\Delta W = \sum_i c_i \sigma^{n_i}$$

Various values of c_1, c_2, etc. will include all the above forms.

In order to study the effect of size in internal damping, consider a prismatical bar freely vibrating. Choose the x-axis along the unstrained position of the neutral axis, the y-axis orthogonal and at the left end of the bar. Ignore the weight of the bar. Then, if m is the mass of the bar per unit length, a differential length, dx, of the bar not at a support can be considered to be acted on by the reversed inertia force $-m\ddot{y}\,dx$. Moreover, if the bar is subjected to a viscous damping force, this force can be added to the reversed inertia force. Let c be the coefficient of viscous damping per unit length of beam so that $-c\dot{y}\,dx$ is the viscous damping force per length, dx, of beam. We find thus for a freely vibrating beam with viscous damping the differential equation of motion

$$(26) \qquad EI\frac{\partial^4 y}{\partial x^4} = -m\ddot{y} - c\dot{y}$$

It is known that internal damping is not viscous. Such damping will be assumed to have its amplitude proportional to some power of the amplitude of the bending moment. Under this assumption, the energy dissipated per cycle per unit length can be expressed in the form

$$(27) \qquad \text{Energy dissipated} = \alpha X''^{\mu}$$

where μ is a constant and X'' is proportional to the amplitude of the bending moment. We can now compute an equivalent viscous damping coefficient, c_{eq}, on the assumption that the energy dissipated by the viscous damping is the same as that dissipated by the internal damping. Thus

$$\alpha X''^{\mu} = \pi c_{eq} X^2 \omega \tag{28}$$

or

$$c_{eq} = \frac{\alpha X''^{\mu}}{\pi \omega X^2} \tag{29}$$

where ω is the circular frequency of the vibration

α is a constant depending on the magnitude of the internal damping

c_{eq} is the coefficient of equivalent viscous damping

X is the amplitude of vibration

and X'' is the amplitude of the curvature of the beam.

Substitution of Eq. (19) in Eq. (26) yields the equation of motion for free vibration with internal damping:

$$EI \frac{\partial^4 y}{\partial x^4} = -m\ddot{y} - \frac{\alpha X''^{\mu}}{\pi \omega X^2} \dot{y} \tag{30}$$

The mass, m, per unit length of beam is $\frac{\gamma A}{g}$ where γ is specific weight, A is cross sectional area, and g is gravitational acceleration. With this substitution Eq. (30) becomes

$$EI \frac{\partial^4 y}{\partial x^4} = -\frac{\gamma A}{g} \ddot{y} - \frac{\alpha X''^{\mu}}{\pi \omega X^2} \dot{y} \tag{31}$$

Define:

$x = L\xi$ where L is a characteristic length

$y = L\eta$

$t = \frac{L\tau}{a}$

$A' = L^2 s$

$k = L\kappa$ (k is the radius of gyration)

$\omega = \frac{a\Omega}{L}$

$\frac{\alpha X''\mu}{\pi E X^2} = q$

$a = \sqrt{\frac{Eg}{\gamma}}$

In any one cycle q can be considered to be constant, depending only on the values of X and X'' at the beginning of the cycle.

Since $\frac{\partial^n y}{\partial x^n} = L^{1-n}\frac{\partial^n \eta}{\partial \xi^n}$ and $\frac{\partial^n y}{\partial t^n} = a^n L^{1-n}\frac{\partial^n \eta}{\partial \tau^n}$ Eq. (31) can be put into dimensionless form:

(32) $$\kappa^2 \frac{\partial^4 \eta}{\partial \xi^4} = -\frac{\partial^2 \eta}{\partial \tau^2} - \frac{g}{s\Omega}\frac{\partial \eta}{\partial \tau}$$

where all the quantities are dimensionless.

To solve Eq. (32) assume a solution of the form

(33) $$\eta = \Xi(\xi)\,T(\tau)$$

Then
$$\kappa^2 T \frac{\partial^4 \Xi}{\partial \xi^4} = -\Xi\frac{\partial^2 T}{\partial \tau} - \frac{g}{s\Omega}\,\Xi\,\frac{\partial T}{\partial \tau}$$

whence

(34) $$\kappa^2 \frac{\partial^4 \Xi}{\partial \xi^4} = c\,\Xi$$

and

(35) $$\frac{\partial^2 T}{\partial \tau^2} + \frac{g}{s\Omega}\frac{\partial T}{\partial \tau} + cT = 0$$

The solution of Eq. (34) is seen to be

(36) $$\Xi(\xi) = a_1 \cosh p\xi + a_2 \sinh p\xi + a_3 \cos p\xi + a_4 \sin p\xi$$

where $$p = \sqrt[4]{\frac{c}{k^2}}$$

The solution of Eq. (35) will be assumed to be of the form

(37) $$\bar{T} = \bar{A}_0 e^{i\Omega\tau}$$

where $\bar{A}_0 = A_0 e^{i\beta}$. The real part of T will then give the desired solution. Then

$$-\Omega^2 + \frac{g i}{s} + c = 0$$

or

(38) $$\Omega = \sqrt{c + \frac{g i}{s}}$$

We observe, by considering Eq. (35) with the middle term deleted, that

(39) $$c = \Omega_n^2$$

where Ω_n is the dimensionless natural frequency.

Hence, if we set

(40) $$\epsilon = \frac{g}{s\Omega_n^2}$$

then

(41) $$\Omega = \Omega_n(1 + \epsilon i)^{\frac{1}{2}}$$

or, if $\epsilon \ll 1$

(42) $$\Omega = \Omega_n(1 + \tfrac{1}{2}\epsilon i)$$

This done we can rewrite Eq. (37) in the form

$$\bar{T} = \bar{A}_o e^{i\Omega_n(1+\frac{1}{2}\epsilon i)\tau}$$

$$\bar{T} = A_o e^{-\frac{1}{2}\epsilon\Omega_n\tau}\left[\cos(\Omega_n\tau+\beta) + i\sin(\Omega_n\tau+\beta)\right]$$

and the solution which we seek becomes

(43) $$T = A_o e^{-\frac{1}{2}\epsilon\Omega_n\tau}\cos(\Omega_n\tau+\beta)$$

The exponent $\epsilon\Omega_n$ can be rearranged through the use of Eq. (39). Thus

(44) $$\epsilon\Omega_n = \frac{g}{s\Omega_n^2}\Omega_n = \frac{g}{s\Omega_n}$$

Whence, finally, we obtain as the expression for T

(45) $$T = A_o e^{-\frac{g}{2s\Omega_n}\tau}\cos(\Omega_n\tau+\beta)$$

The solution can now proceed in the usual fashion. Equation (36), together with the boundary conditions will yield a frequency equation, thus determining a sequence of values for c: c_1, c_2, c_3, ... Each value of c_1 will yield by Eq. (39) a corresponding value of Ω_n : $\Omega_{n_1}, \Omega_{n_2}$, ... The general solution of Eq. (32) then is

(46) $$\eta = \sum_{i=1}^{\infty}(a_1\cosh p_i\xi + a_2\sinh p_i\xi + a_3\cos p_i\xi + a_4\sin p_i\xi)\cdot$$
$$\cdot A e^{-\frac{g}{2s\Omega_{n_i}}\tau}\cos(\Omega_{n_i}\tau+\beta)$$

where $p = \sqrt[4]{\frac{c_i}{k^2}}$, $\Omega_{n_i} = \sqrt{c_i}$, and $\frac{g}{s\Omega_{n_i}^2} << 1$.

For any given mode, the ratio of two consecutive amplitudes is

(47) $$\frac{\eta_{i_m}}{\eta_{i_{m+1}}} = e^{\frac{\pi q}{s \Omega_n^2}}$$

and the logarithmic decrement is

(48) $$L.D. = \frac{\pi q}{s \Omega_{n_i}^2}$$

Returning to the expression for q, we find that

(49) $$L.D. = \frac{\alpha X_m''^{\mu}}{E s X_m^2 \Omega_{n_i}^2}$$

From Eq. (49) we conclude that the logarithmic decrement decreases with time. The curvature, X_m'', will approach zero with the amplitude, X_m. Since μ is known from experience to be greater than 2, the ratio $X_m''^{\mu}/X_m^2$ will become arbitrarily small.

A further remark about the logarithmic decrement is necessary because the presence of Ω_{n_i} in the denominator of Eq. (49) conveys the impression that the higher frequency modes will not be damped out as rapidly as are the modes of lower frequency.

This is not a correct conclusion as can be shown by writing X_m in dimensionless form. For the i-th mode

(50) $$X_m = L \eta_{i_m} = L \Xi f(\tau)$$

since throughout the m - th cycle T (τ) is a function of τ only. Consequently

$$X_m'' = \frac{1}{L} f(\tau) \frac{\partial^2 \Xi}{\partial \xi^2}$$

$$= \frac{1}{L} f(\tau)\, p_i^2 (a_1 \cosh p_i \xi + - - - - - a_4 \sin p_i \xi)$$

Replacing p_i^2 by $\frac{\Omega_{n_i}}{k}$ leads to

(51) $$L.D. = \frac{\alpha f(\tau)^{\mu-2} (a_1 \cosh p_i \xi + - - - - - - a_4 \sin p_i \xi)^{\mu}}{k^{\mu} E S L^{\mu+2} (a_1 \cosh p_i \xi + \cdots + a_4 \sin p_i \xi)^2} \Omega_{n_i}^{\mu-2}$$

Consider now the variation of α with size of beam. α is defined by Eq. (27) in such a way that $\alpha X''^{\mu}$ is the energy dissipated per cycle in length, dx, of the beam.

A brief consideration of the dimensions of the variables involved in hysteresis damping reveals that if we assume the energy thus dissipated, E.D., to depend only on the maximum stress, σ , and on the maximum strain, ϵ , then

$$E.D. = \sum_i c_i \sigma \epsilon^{\nu_i}$$

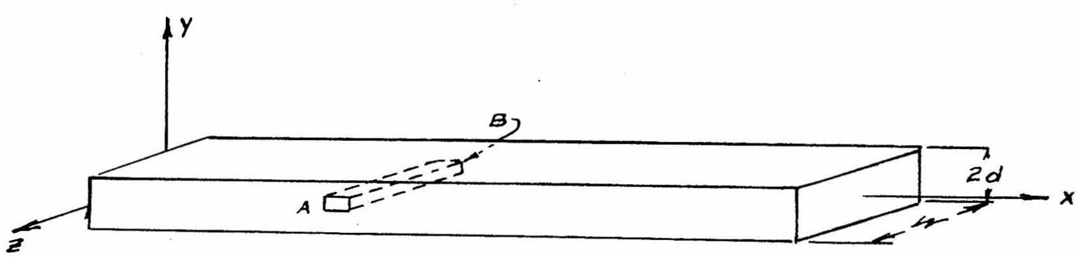

Fig. 3

In particular suppose that the beam shown in Fig. 3 is vibrating in the x-y plane and that the displacement of the neutral axis is given by

(52) $$y = \sum_{i=1}^{\infty} X_i\, q_i(t)$$

where X_i is the eigen-function for the i-th mode of vibration of the beam. Let t_m and t_{m+1} be successive values of t which maximize $g_i(t)$. For the fiber AB of axial dimension dx and depth dimension dh lying a distance h from the beam's neutral axis, its maximum stress in the m-th cycle of the i-th mode is $E h X_i'' q_i(t_m)$ and the corresponding maximum strain is $h X_i'' q_i(t_m)$.

(In the following we shall assume that c_i is zero for all i save i = 1. This is done only to simplify the notation. The extension of the conclusions to more general assumptions on c_i is immediate.)

The energy dissipated E.D.' by a transverse lamina of thickness dx in one cycle is then

$$E.D.' = 2\int_{h=0}^{h=d} c_1\, w\, dx \left[E h X_i'' q_i(t_m)\right]\left[h X_i'' q_i(t_m)\right]^{\nu} dh$$

or

$$E.D.' = c_1 E w d^{\nu+2} X_i''^{\nu+1} \left[q_i(t_m)\right]^{\nu+1} dx \tag{53}$$

Comparing Eqs. (53) and (27) leads to

$$\alpha = c_2 E w d^{\nu+1} \tag{54}$$

or, since wd = A,

$$\alpha = c_2 E A d^{\nu} \tag{55}$$

where A is the cross-sectional area of the beam and d is its half depth.

Writing $d = L\delta$ and $A = L^2 s$ brings Eq. (51) into the form

$$L.D. = \frac{c\,\delta^{\mu} f(\tau)^{\mu+2} (a_1 \cosh p_i\xi + \cdots\cdots - a_4 \sin p_i\xi)^{\mu}}{k^{\mu} (a_1 \cosh p_i\xi + \cdots\cdots + a_4 \sin p_i\xi)^2}\, \Omega_{n_i}^{\mu-2} \tag{56}$$

where all quantities are dimensionless. We would then expect to be able to model internal damping.

This conclusion can be supported, as well, on energy considerations. Making the usual substitutions, namely,

$x = L\xi, \quad w = L\beta, \quad d = L\delta, \quad X'' = L^{-1}\Xi'', \quad t = \frac{L\tau}{a}$

leads to

$$(57) \qquad E.D.' = c E \delta^{\nu+2} L^3 \Xi''^{\nu+1} [q_i(t_m)]^{\nu+1} d\xi.$$

as the expressions for the energy dissipated by a lamina of length d in the m-th cycle of the i-th mode. The total energy dissipated by the beam in this cycle of this mode is

$$(58) \qquad E.D. = \int_0^1 E.D.' d\xi = c E \delta^{\nu+2} L^3 [q_i(t_m)]^{\nu+1} \int_0^1 \Xi_i''^{\nu+1} d\xi$$

The maximum potential energy of bending in the m-th cycle of the i-th mode is

$$(59) \qquad P.E. = \frac{EI}{2} \int_0^L [X_i'' q_i(t_m)]^2 dx = \frac{2\beta\delta L^2 E}{2} L^3 [q_i(t_m)]^2 \int_0^1 \Xi_i''^2 d\xi.$$

Realizing that the maximum potential energy occurs when the kinetic energy is zero leads to the equation

$$(60) \qquad E\beta\delta L^3 \int_0^1 \Xi_i''^2 d\xi \left[q_i^2(t_m) - q_i^2(t_{m+1})\right]$$
$$= c E \delta^{\nu+2} L^3 \int_0^1 \Xi_i''^{\nu+1} d\xi \, [q_i(t_m)]^{\nu+1}$$

which merely states that the difference in maximum potential energy in two successive cycles equals the energy dissipated during the cycle.

The substitution of $L\tau/a$ for t in Eq. (60) reduces the equation to dimensionless form except for the E and L^3 which appear on both sides of the equation. It immediately follows that for two beams which are geometrically similar and have the same boundary and initial conditions, the effect of damping can be correctly modeled.

SUMMARY OF CONCLUSIONS:

The conclusions reached in the foregoing analysis can be summarized for convenience.

(A) If damping be ignored, the free vibration of a beam whose statical deflection curve is $y = f(x,0)$ and which has an initial velocity $\dot{y} = v(x,0)$ can be modeled if

$$\left(\frac{k}{L}\right)_{Prototype} = \left(\frac{k}{L}\right)_{Model}$$

$$\left(\frac{f(x,0)}{L}\right)_{Prototype} = \left(\frac{f(x,0)}{L}\right)_{Model}$$

$$\left(\frac{v(x,0)}{a}\right)_{Prototype} = \left(\frac{v(x,0)}{a}\right)_{Model}$$

where k = radius of gyration

L = length of beam

a = rate of propagation of small elastic waves.

(B) In order to model a beam acted on by a concentrated forcing function, P, of the type P = p sin Ω t the conditions in addition to those given in (A) above, which must be satisfied are

$$\left(\frac{\Omega L}{a}\right)_{Prototype} = \left(\frac{\Omega L}{a}\right)_{Model}$$

$$\left(\frac{P}{\gamma a^2 L^2}\right)_{Prototype} = \left(\frac{P}{\gamma a^2 L^2}\right)_{Model}$$

$$\left(\frac{A}{L^2}\right)_{Prototype} \qquad \left(\frac{A}{L^2}\right)_{Model}$$

where a and L are as defined in (A)

γ = specific weight of the material

A = cross-sectional area of the beam.

(C) In order to model a beam whose root is subjected to an acceleration f(t) given by

$$f(t) = 0 \quad \text{if} \quad t \leq 0$$

$$f(t) = b \sin \omega t \quad \text{if} \quad 0 \leq t \leq \frac{\pi}{\omega}$$

$$f(t) = 0 \quad \text{if} \quad \frac{\pi}{\omega} \leq t$$

the conditions, in addition to those given in (A) above, which must be satisfied are:

$$\left(\frac{Lb}{a^2}\right)_{Prototype} = \left(\frac{Lb}{a^2}\right)_{Model}$$

$$\left(\frac{L\omega}{a}\right)_{Prototype} = \left(\frac{L\omega}{a}\right)_{Model}$$

where a and L are as defined in (A).

(D) In order to model a beam subjected to a uniformly distributed forcing function $U(t) = \frac{P}{L} \sin \omega t$ by means of an acceleration $b \sin \omega t$ applied to its root, b must satisfy the relationship $b = -\frac{gP}{\gamma A L}$ and the conditions given under (A) and (C) must be observed.

(E) In order to model a beam whose root is given an acceleration of short duration, k/L must be the same for both prototype and model and the ~~acceleration~~ impulse must also be the same for each.

(F) The effect of internal damping can be satisfactorily modeled through the use of geometrically similar models of the same material.

CHAPTER II

The theory developed in Chapter I was subjected to experimental verification. Three tests were conducted:

(1) Bars of a variety of sizes and shapes were mounted as cantilever beams. Each was given an initial deflection. The load producing the deflection was suddenly removed and the strain in the beam as a function of time was observed. The object of this test was to observe the effect of damping on the free vibration of the beam.

(2) Three cantilever beams, modeled according to the conditions established by the theory had their roots simultaneously subjected to the same acceleration of short duration. The strains developed in the beams were recorded. The object of this test was to observe the effect of damping in this type of vibration and to determine the range over which the duration of the acceleration can be considered to be very short.

(3) Six cantilever beams had their roots subjected to continuing sinusoidal acceleration. The amplitude of the acceleration was modeled in accordance with the theory. The object of this test was to verify the theory and to show that internal damping can be modeled.

The apparatus and procedures used for these tests are described in detail in this chapter.

FREE VIBRATION TESTS:

Beams of the sizes and shapes shown in Fig. 4 were fabricated. Electric resistance strain gages (SR-4 Type C-1) were attached on opposite sides of each beam at a point $\frac{9}{10}$ of its free length from its free end. A vise shown in Fig. 5 was fabricated and rigidly attached to a reinforced concrete slab floor, 12 inches thick. The construction details of the vise are shown in Fig. 6.

Test 1. (a) Each of the beams was clamped in the vise as shown in Fig. 7 and the nuts were tightened with a torque wrench. The free end of each beam was deflected by means of a length of piano wire (B.S. gage No. 28) until the strain under the gages was 300 micro inches per inch. This strain was measured by a Baldwin Southwark Type K Strain Indicator.

(b) The deflection of the free end was measured by a dial indicator as shown in Fig. 7. The deflection of the dial indicator stand due to the change in the spring load of the dial indicator as its plunger moved out with the deflection of the end of the beam was observed by means of a transit and was found to be of the order of 0.00010 inches. This was considered to be negligible in subsequent work. From the observed deflection and the geometry of each beam, the strain under the gages was computed. This was found to be in all cases 300 $\pm$ 8 micro inches per inch. It was concluded that the vise was sufficiently rigid so that a clamped end for the beam was effectively obtained.

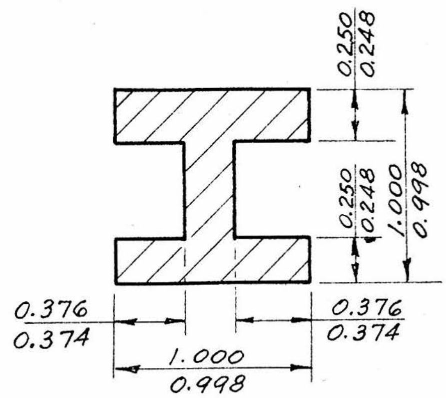

Beam No.	Free Length*	Material
1	30 in.	Aluminum
4	30 in.	Brass
21	30 in.	Steel (Cold Rolled)

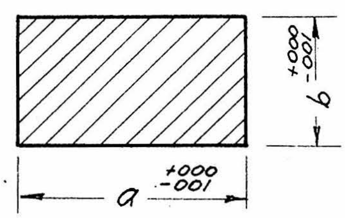

Beam No.	Free Length* (in.)	a (in.)	b (in.)	Material
3	24.80	0.997	0.997	Aluminum
11	12.42	1.000	0.499	Aluminum
12	18.62	1.500	0.750	Brass
13	9.23	1.000	0.372	Brass
15	7.82	0.750	0.312	Cold Rolled Steel
16	12.42	1.000	0.499	Cold Rolled Steel
17	12.42	1.498	0.499	Cold Rolled Steel
30	40.00	0.998	0.998	Cold Rolled Steel
31	20.00	0.498	0.498	Cold Rolled Steel

Fig. 4

---

* Each beam was 2 inches longer than the free length to allow for clamping.

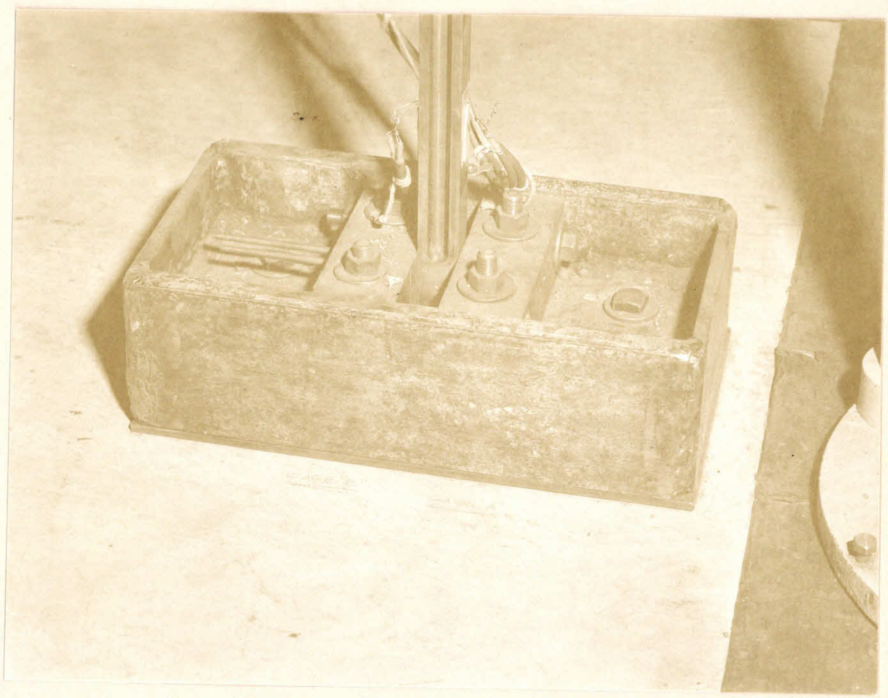

Fig. 5.

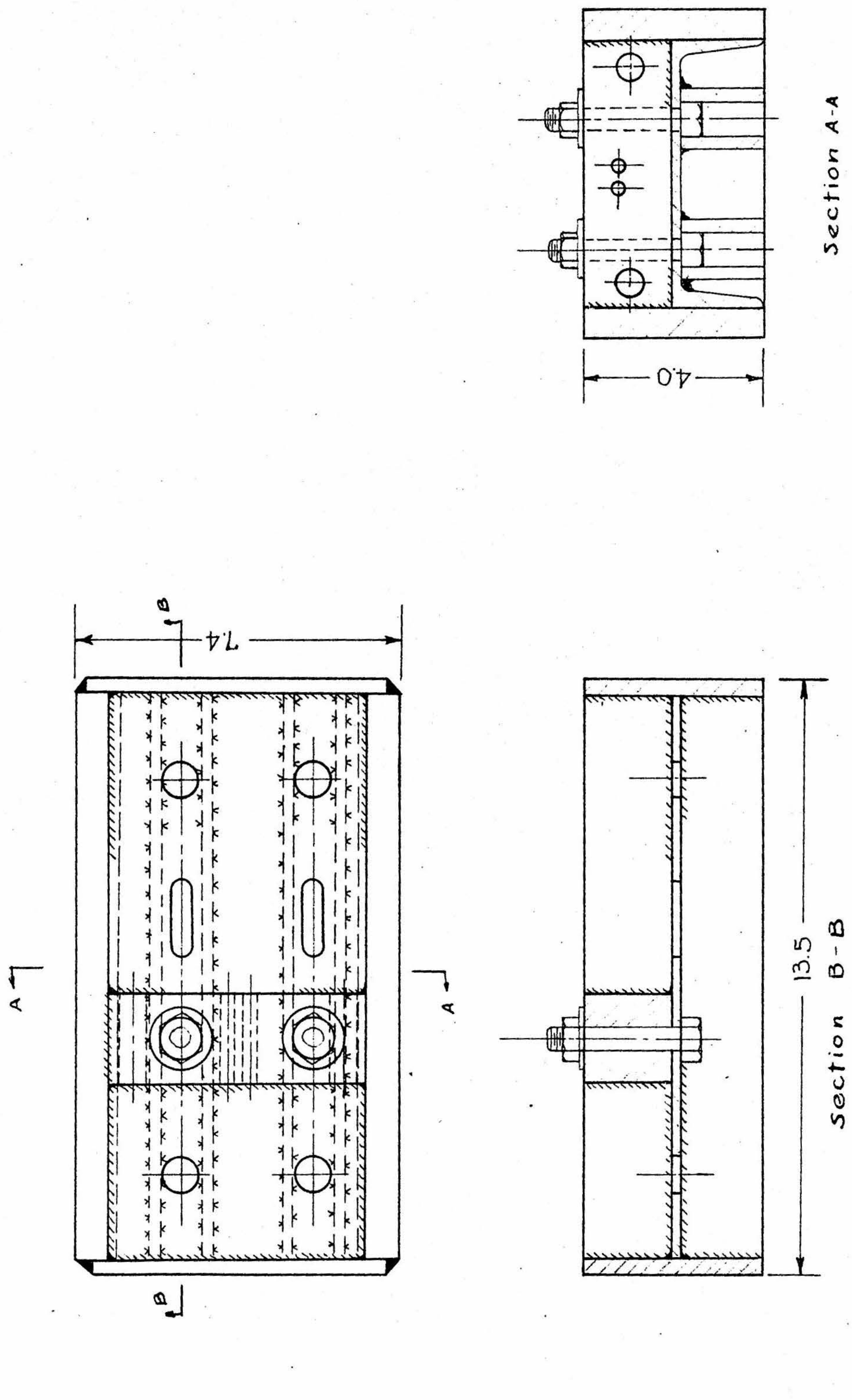

Fig. 6. Detail of Vise.

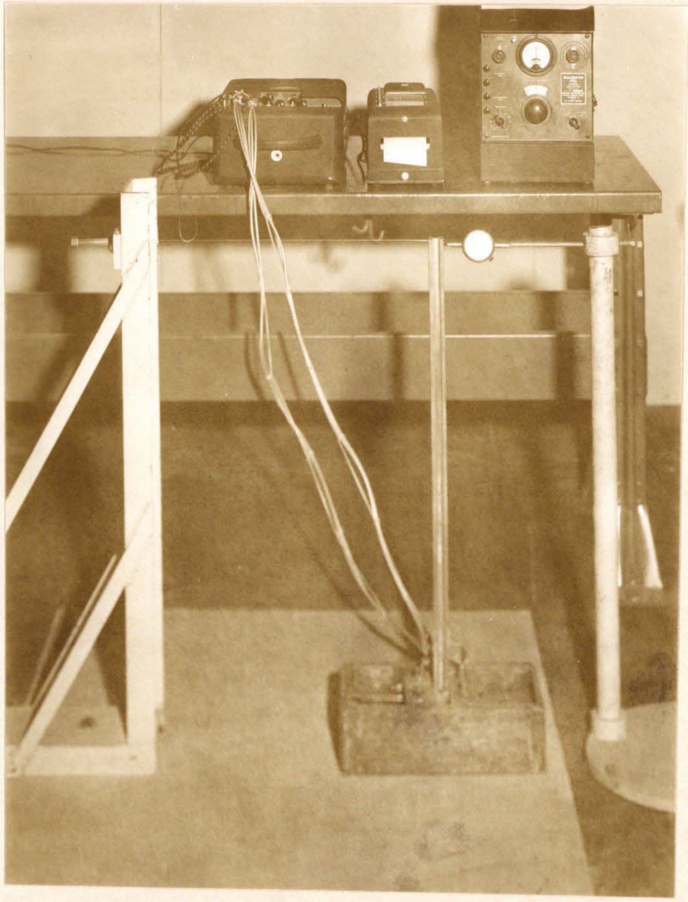

Fig. 7.

(c) The deflection of the free end of the beam by means of the piano wire proved onerous. Investigations were undertaken seeking to simplify the procedure. The wire was subsequently replaced by a strut of maple, 1/2 inch in diameter inserted between the stand shown at the left of Fig. 7 and the free end of the beam. The end of the strut at the left was cut off perpendicular to the axis of the strut and was butted against a screw in the stand for adjusting the deflection. The right end of the strut was rounded so as to give point contact against the beam. When the piano wire was used to produce the deflection of the free end of the beam, the load was suddenly released by cutting the wire. When the deflection was produced by the strut, a fast upward sweep of the investigator's hand suddenly removed the strut and released the load. Strain vs. time curves for the two methods were indistinguishable.

(d) For Beams Nos. 1, 3, 4, 12, 13, and 21, with the beam deflected as in Part (c) the strain gages were connected to a Brush Type BL-310 strain analyzer. The strut producing the deflection of the beam was removed and the beam was allowed to vibrate freely. The variation of strain under the gages with time was recorded. This method could not be used with Beams Nos. 11, 15, 16 and 18, because their natural frequencies were beyond the range of response of the Brush instrument. Their strain variation as a function of time was recorded as outlined in Part (e) immediately following.

(e) To record the strain decay curves for Beams Nos. 11, 15, 16, and 17, a DuMont Oscilloscope Type 208-B, with a Type P-11 tube and a Fairchild Recording Camera were used. Eastman Panatomic X or Plus X film was used. A signal of 164 cycles per second and an amplitude on the oscilloscope screen of 2 inches either side of center was found to record satisfactorily on Panatomic X with an aperture of f:2.8 and a film speed up to 30 inches per second. Tank development was in Eastman developed DK 60-a for 12 minutes at a temperature of 68° F. Higher film transport speeds were not investigated. For Plus X film, correspondingly smaller apertures were used. Because the Fairchild camera provides only vertical film transport, the x- and y-axes of the oscilloscope were interchanged for this work in order to gain the advantages of the y-axis amplifier for a screen image with a horizontal displacement only. The interchange of axes is easily accomplished by interchanging leads on the back of the oscilloscope. In recording the strains for these beams the bridge circuit shown in Fig. 8 was used.

The oscilloscope provided insufficient gain in its y-axis amplifier for this bridge circuit. Consequently a pre-amplifier was constructed. The circuit diagram of this pre-amplifier is shown in Fig. 9 and its response curves are shown in Fig. 10. The frequency response curve of the oscilloscope is shown in Fig. 11.

Beam 12 was installed in the vise and subjected to a strain decay test as in Part (d) above, the curve of strain

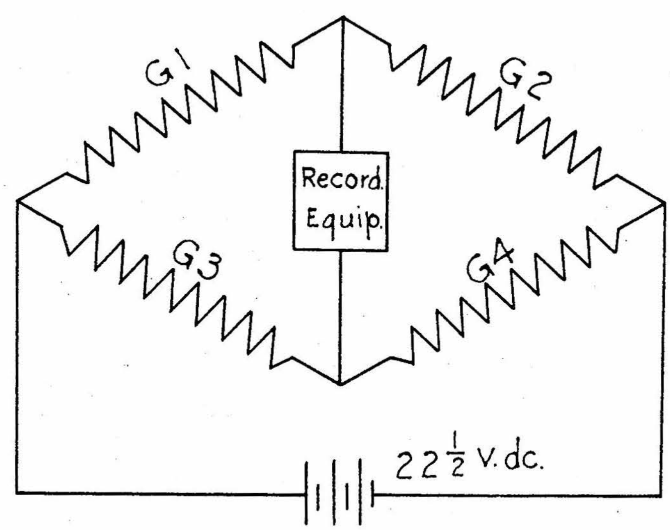

Fig. 8. Bridge Circuit. Gages G1 and G2 on test structure. Gages G3 and G4 on unstrained structure of same material as test structure and subject to same ambient temperature. All gages SR-4. Type C-1.

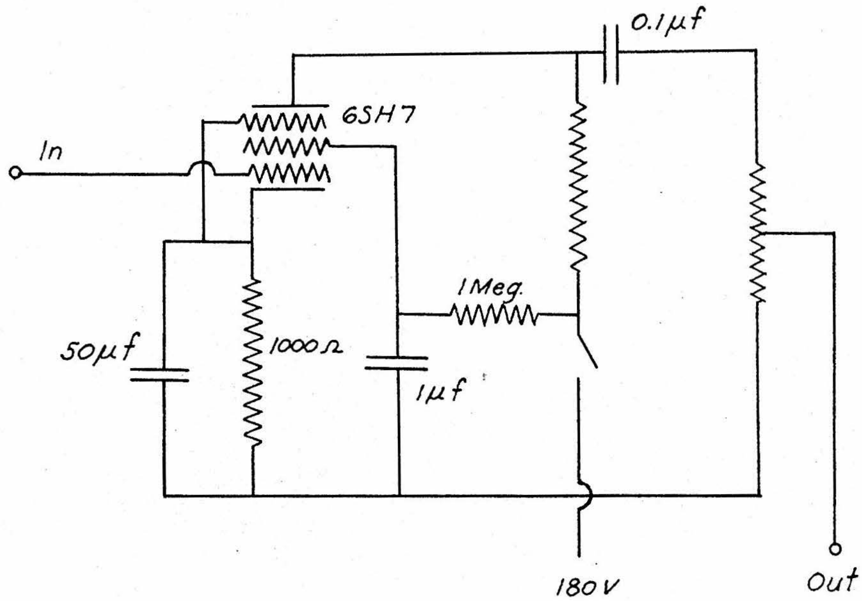

Fig. 9. Amplifier Circuit.

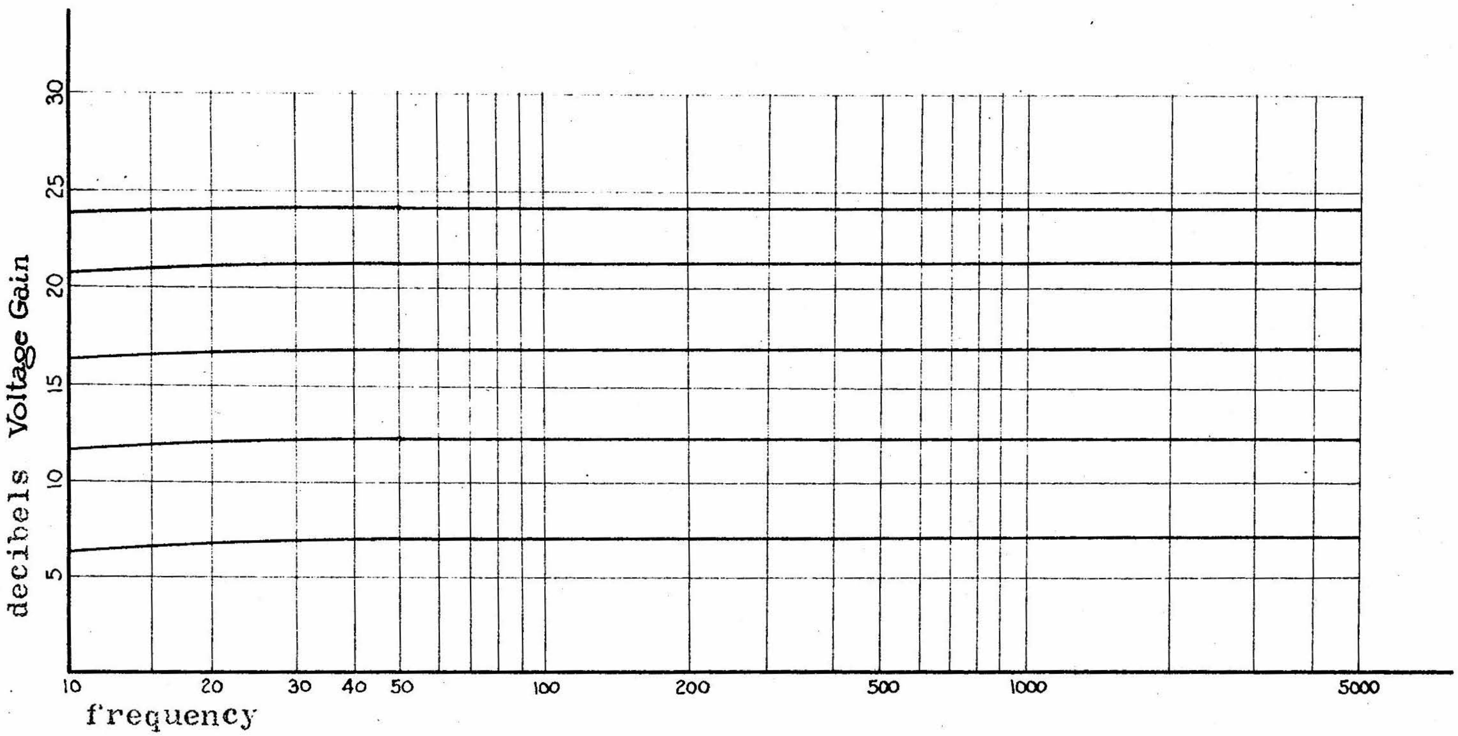

Fig. 10. Frequency Response of Amplifier.

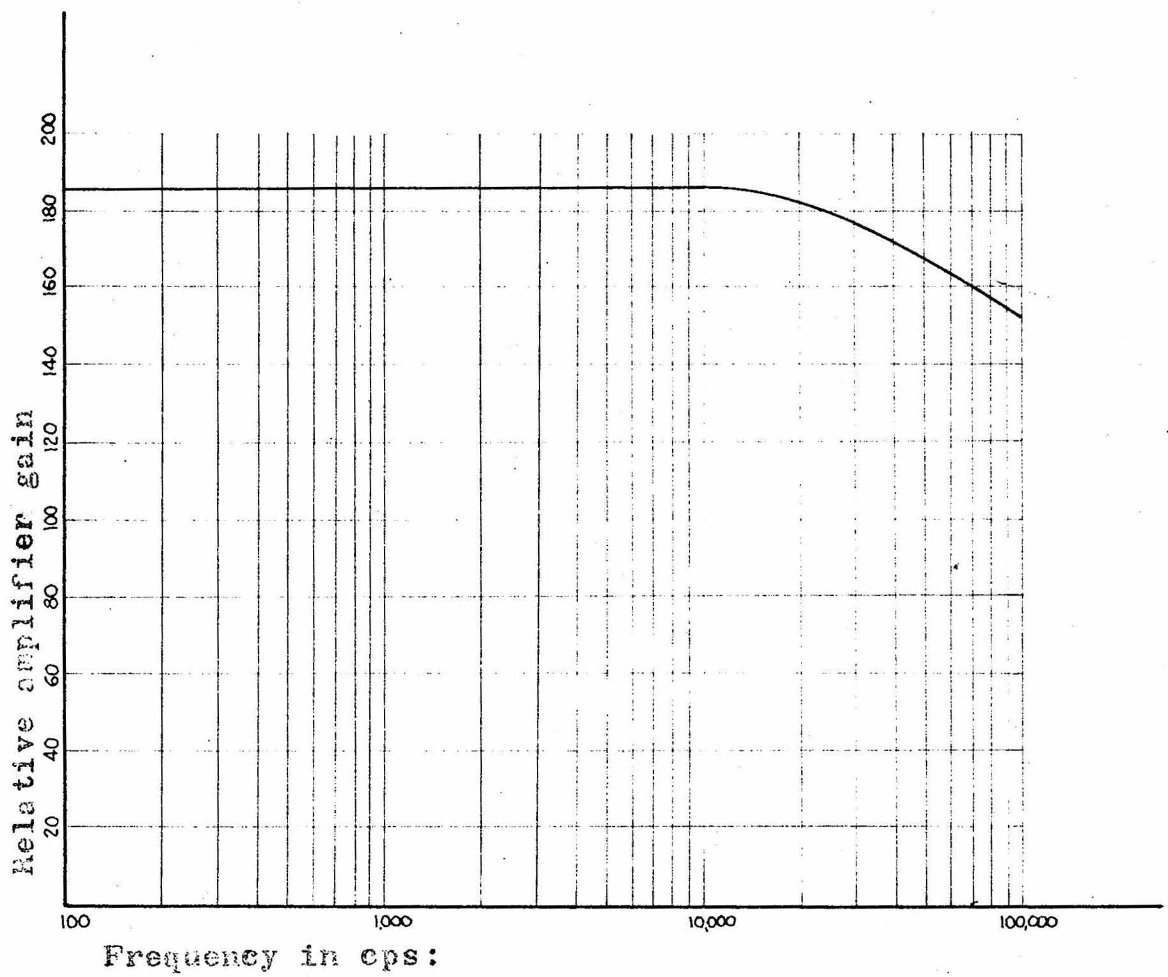

Fig. 11. Frequency response of DuMont Type 208-B Oscilloscope

vs. time being recorded by the Brush equipment. The same test was repeated but this time the record was made with the oscilloscope circuit. Beams Nos. 11, 15, 16 and 17 were then subjected to strain decay tests and their strain vs. time curves were recorded by means of the oscilloscope camera.

(f) In order to evaluate the effect of external damping as contrasted to internal damping in the foregoing strain decay tests, additional investigations were undertaken. The tests outlined in Part (d) above were repeated with Beams 30 and 31 with the vise as constructed. Malleable copper jaws were then inserted between the jaws of the vise and the root of the beam. It was found that this increased the damping slightly, (i.e. the dynamic strains were decreased by about 10 percent.) The use of copper jaws was abandoned. Next the entire vise was suspended by means of a fine wire (piano wire, B.S. gage No. 28) from an overhead support as shown in the photograph of Fig. 12. Strain decay curves were again recorded. It was found that the curves differed by $\pm$ 5 percent from those obtained with the vise secured to the floor.

(g) The frequency of each beam was observed by means of a General Radio Strobotac. Through the use of a variable speed motor, the strobotac was calibrated before each test by comparing it against a revolution counter and stop watch.

Fig. 12.

IMPULSE TESTS:

Beams of the size and shape shown in Fig. 13 were fabricated. A vise constructed as shown in Fig. 14 was prepared for attachment to a drop table. SR-4 Strain Gages were then applied on opposite sides of each beam at a position 9/10 of the free length of the beam from the free end. An accelerometer made by Statham Instrument Company was attached to the drop table. The drop table was allowed to fall freely through a distance of 1 ft. and was suddenly brought to rest by striking a round lead strut. The stresses developed in the beams and the acceleration were recorded by means of Consolidated Recording Oscillograph Equipment. Since only the relative values of the stresses were of importance, the maximum stress developed in each beam was not calibrated although the relative values of the three maximum stresses were calibrated by interchanging the channels on which the recordings were made. Likewise, no attempt was made to calibrate the magnitude of the acceleration since only its duration was of importance.

FORCED VIBRATION TESTS:

Beams of the sizes and shapes shown in Fig. 15 were fabricated. Beams Nos. 32, 33 and 34 were all cut from the same piece of bar stock which was hot rolled SAE 1025 steel, 1-1/4" x 6" x 34". These pieces were milled to 1/8" of size in all dimensions and were simultaneously annealed, being soaked at a temperature of 1450° F for two hours and allowed

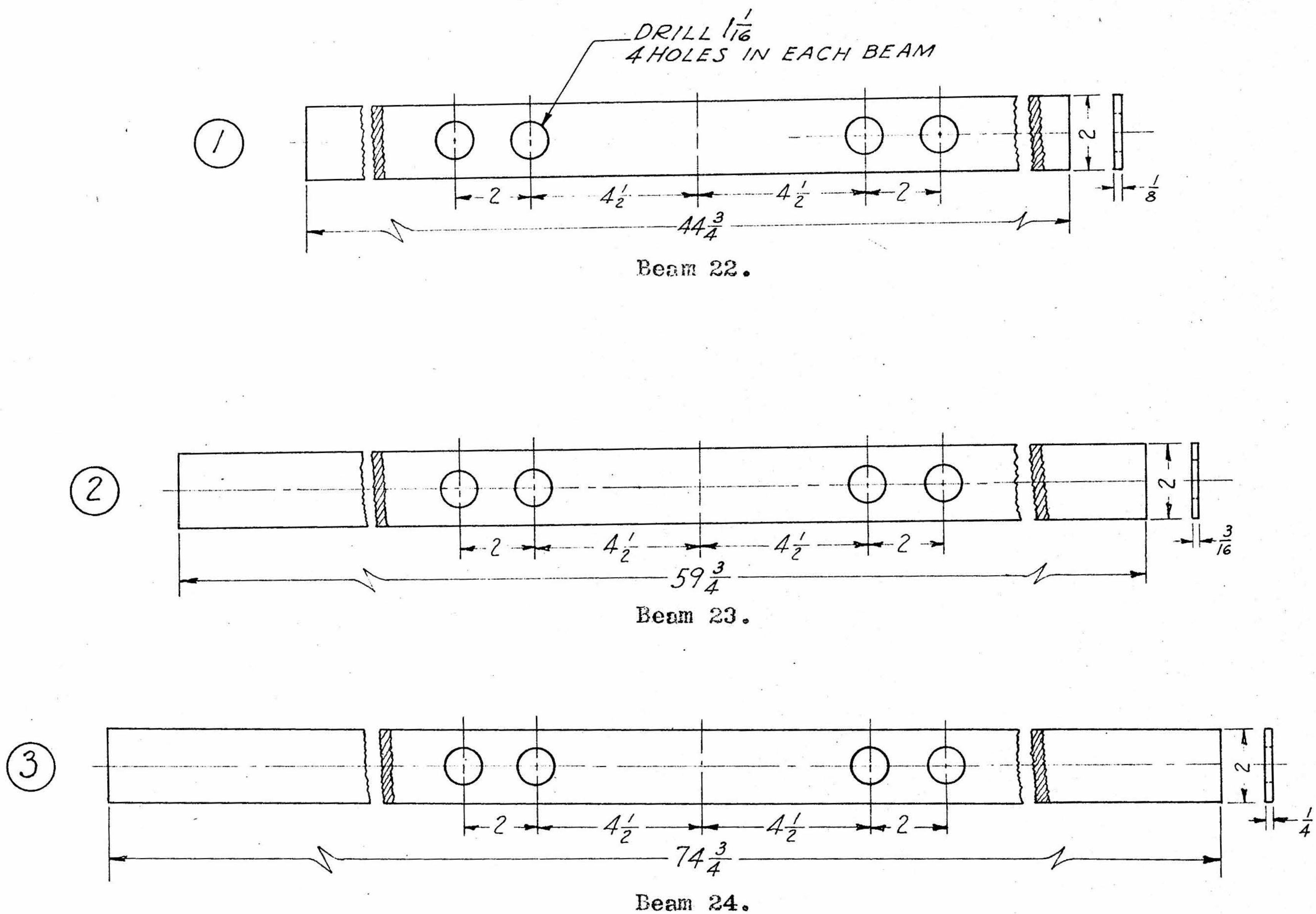

Fig. 13. Beams for Impulse Test.

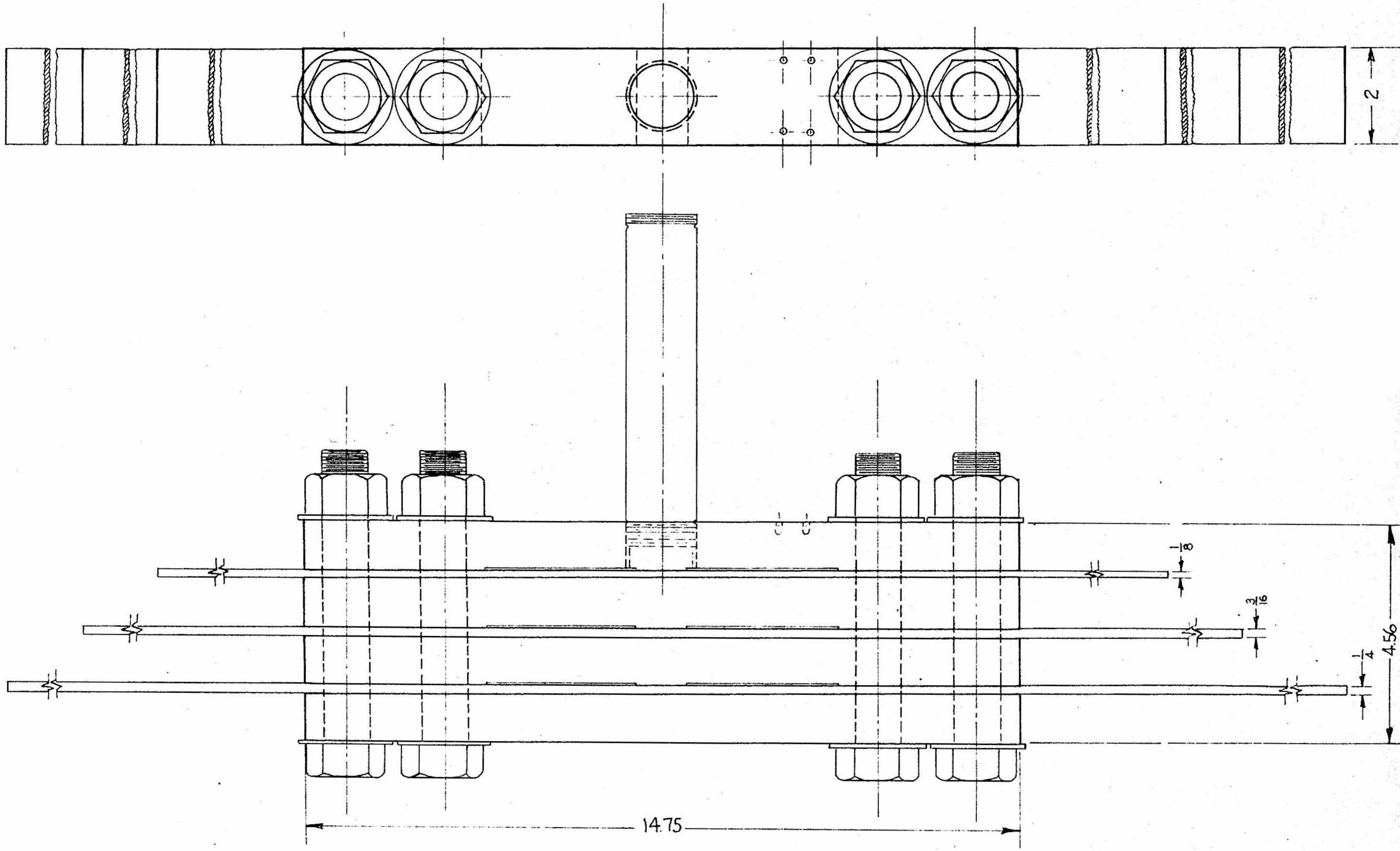

Fig. 14. Vise for Impact Tests

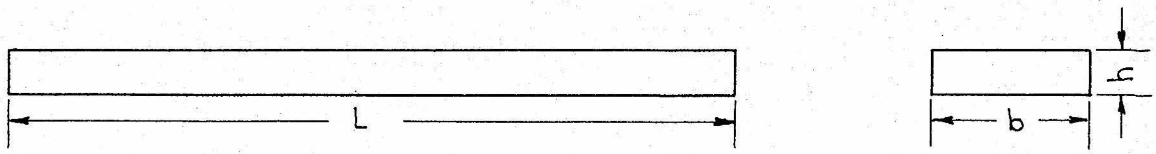

Beam No.	L	b	h	Material
32	$30 \pm 1/64$	$\frac{2.000}{1.999}$	$\frac{1.000}{0.999}$	SAE 1025 Ht. Tr.*
33	$22\frac{1}{2} \pm 1/64$	$\frac{1.500}{1.499}$	$\frac{0.750}{0.749}$	SAE 1025 Ht. Tr.*
34	$15 \pm 1/64$	$\frac{1.000}{0.999}$	$\frac{0.500}{0.499}$	SAE 1025 Ht. Tr.*
35	$30 \pm 1/64$	$\frac{2.000}{1.997}$	$\frac{1.000}{0.997}$	SAE 1025 Cold Rolled
36	$22\frac{1}{2} \pm 1/64$	$\frac{1.500}{1.497}$	$\frac{0.750}{0.747}$	SAE 1025 Cold Rolled
37	$15 \pm 1/64$	$\frac{1.000}{0.997}$	$\frac{0.500}{0.497}$	SAE 1025 Cold Rolled

* Beams 32, 33, 34 to be cut from same piece of stock, SAE 1025 Hot Rolled. Anneal at 1450° F. Soak for 2 hours. Furnace cool 12 to 16 hours.

Fig. 15.

to furnace cool for fourteen hours. Each of the three beams showed a Brinnell hardness of 55.0 with a 10 mm. ball and 3000 Kg. load. Only Beam No. 33 showed any warp under this treatment. It bowed in a direction perpendicular to 1" x 22-1/2" face, an amount of 3/32 of an inch. It was subsequently press straightened. All three beams were then surface ground to the required dimension with a surface finish of abpit 50 micro-inches RMS. SR-4 Type Strain Gages were then mounted on opposite sides of the six beams (Beams Nos. 32-37) at a position 9/10 of the free length from the free end of the beam. A vibrating stand assembly as shown in Fig. 16 was designed and fabricated. The stand consists of a heavy base, a fixed-fixed beam which is used as a spring, and a Lazan oscillator which constitutes a mass. The oscillator is driven as shown by pulleys and a V-belt from a 1 H.P. electric motor through a Graham variable speed drive. The range of speed for the vibration stand is from 0 to 3750 r.p.m. The Lazan oscillator generates a maximum forcing function of plus or minus 1650 lbs. and an assortment of fixed-fixed beams ranging in thickness from 5/16 to 1/2 is provided by interchanging these fixed-fixed beams. Amplitudes of the vibration shaking table as great as plus or minus 1/2" are available. For heavy test structures the various beams can be used in combination to give greater spring constant. The displacement of the shaking table is sinusoidal although it is essential that test structures be dynamically balanced

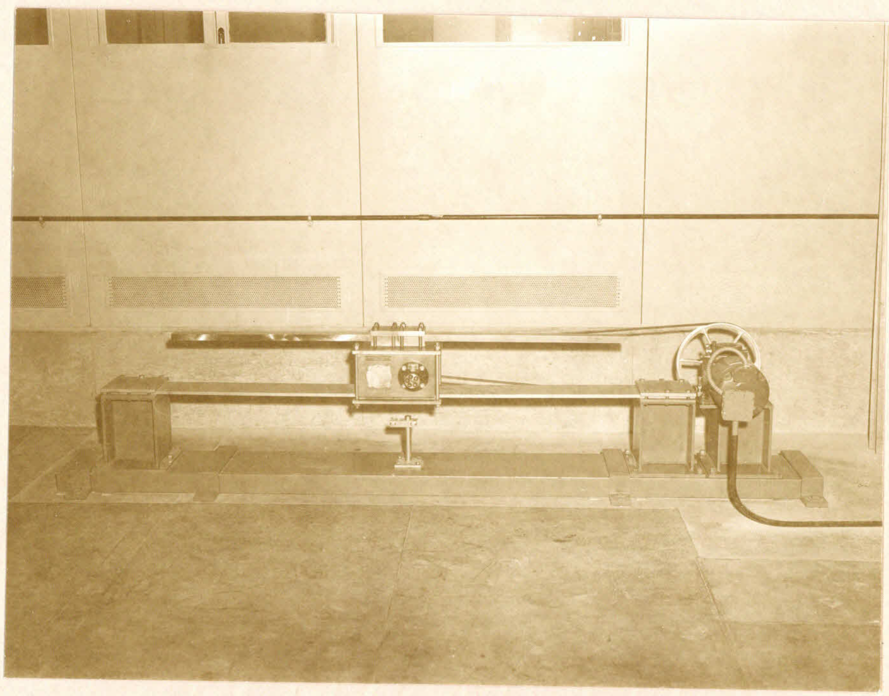

Fig. 16.

on either side of the center line of the shaking table. Otherwise the fixed-fixed beam is apt to begin vibrating in an unsymmetric mode.

Beams Nos. 32 and 35, 33 and 36, and 34 and 37 were placed successively on the shaking table. The frequency was set at 50 percent of their computed resonant frequencies and the oscillator was adjusted to give sufficient amplitude to cause a strain of 200 micro inches per inch to be developed in Beam No. 32. The beams were vibrated at amplitudes which were in the ratios of 1:3/4:1/2 resp. The strain under the gages was recorded by means of the Brush Strain Gage recorder and by means of the Fairchild oscilloscope recording camera. This was repeated for other frequencies below resonance.

For beams Nos. 32 and 35 the frequency of the shaking table was set at 78.6 percent of the natural frequency of these beams, and the oscillator was adjusted to give sufficient amplitude to cause a strain of 200 micro-inches per inch to be developed in the annealed beam No. 32. The strain under the gage of Beam No. 32 was recorded by means of the Brush equipment and the strain under the gage of Beam No. 35 was recorded by the bridge circuit shown in Fig. 8 and recorded by means of the DuMont oscilloscope and the Fairchild recording camera. Since only relative strain was of interest, the oscilloscope recording was calibrated by interchanging the leads of beams 32 and 35. The amplitude of vibration of the shaking table was observed by means of a dial indicator mounted on the post which appears directly under the oscillator in Fig. 18. The test was continued without interruption at this frequency and amplitude until the beams had been subjected to 1,150,000 cycles of stress.

Beams Nos. 33 and 36 were inserted in the test stand in place of the previous beams. The frequency was set at 78.6 percent of the natural frequency of the beams on the shaking table and the Lazan oscillator was adjusted until the amplitude of vibration of the shaking table was 3/4th of that used for Beams Nos. 32 and 35. The strains developed under the gages were recorded as before. This test was also continued without interruption at this frequency and amplitude until the beams had been subjected to more than 1,100,000 cycles of stress.

The foregoing test was repeated with Beams Nos. 34 and 37 being run at a frequency which was 78.6 percent of their natural frequency and an amplitude of vibration of the shaking table which was 1/2 that used for Beams Nos. 32 and 35. The strains developed under the gages were recorded as before and again the test was continued without interruption at this frequency and amplitude until the beams had been subjected to more than 1,100,000 cycles of stress.

Beams Nos. 32 and 35 were replaced on the shaking table and the frequency was adjusted to their resonant frequency. The amplitude of the shaking table required to produce a strain of 1000 μ in./in. under the gages of Beam No. 32 was observed. The strain in Beam No. 35 was recorded on the Brush equipment. These beams were replaced by Beams Nos. 33 and 36 and the operation was repeated producing a strain of 1000 μ in./in. under the gages of Beam No. 33. The amplitude of the shaking table in the latter case was 27.8 percent of that required for Beams Nos. 32 and 35.

CHAPTER III

DISCUSSION OF RESULTS.

THE FREE VIBRATION TESTS:

Test 1. The dimensionless natural frequency, Ω, of the first mode of vibration of each of the beams listed in Table I was computed by the formula given in Appendix I. The observed natural frequencies are also listed in Table I.

TABLE I

Col. 1	Col. 2	Col. 3	Col. 4	Col. 5	Col. 6
	k	k_0	Ω	f	Ω
Beam No.	Rad. of Gyr. (in.)	Rad. of Gyr. (dimensionless)	(computed)	(Obs.) (Cys/sec)	(Obs.)
1	0.348	0.0116	0.0407	43.6	0.0409
3	0.288	0.0116	0.0407	52.5	0.0410
4	0.348	0.0116	0.0407	27.5	0.0404
11	0.144	0.0116	0.0407	105.3	0.0410
12	0.216	0.0116	0.0407	43.8	0.0404
13	0.107	0.0116	0.0407	88.5	0.0407
15	0.090	0.0116	0.0407	164.0	0.0403
16	0.144	0.0116	0.0407	103.5	0.0404
21	0.348	0.0116	0.0407	42.7	0.0405

NOTE: Observed Ω computed from observed f by means of the formula $\Omega = 2\pi f L/a$. The values of "a" which were used are for steel: 2.00×10^5 in./sec.; for brass: 1.27×10^5 in./sec.; for aluminum: 2.01×10^5 in./sec.

For systems having viscous damping it can be shown that the damped natural frequency is less than the undamped natural frequency.[15] A similar conclusion has not been demonstrated rigorously for systems having internal damping. This want is due to the lack of an analytical solution for the latter problem. A comparison of columns 4 and 6 in Table I seems to lead to such a conclusion since the observed frequency is less than the predicted frequency in most cases. However, this difference is as readily explained on the basis of a variation in the physical properties of the material as by an appeal to the effect of internal damping. There is no need to attempt to use a finer determination of these properties for the model in an effort to distinguish between their effect and that of internal damping. The accuracy of prediction of frequency on the basis of the beams listed in Table I is, moreover, well within the allowable limit set forth in the Introduction. If Beam 15 be considered model and Beam 3 be considered prototype, then the predicted frequency would be 98.5 percent of the observed frequency of the prototype. This represents the greatest inaccuracy in the present test. It should be recalled that Beam 15 is of cold rolled steel, 7.82 inches long and 0.750" x 0.312" in cross section whereas Beam 3 is of aluminum, 24.8" long and 1.997" in cross section. Other, more striking, agreements appear. Again taking Beam 15 as model and Beam 4 as prototype, we find the predicted frequency is 99.6 percent of the observed frequency of the prototype. In this case the model is the same as before but the prototype is a brass H section, 30 inches long, flange width of 1 inch, depth of 1 inch, and flange and web thickness 1/4 inch. (See Fig. 4).

In order to present the strain decay curves with clarity it is necessary to define a dimensionless unit of time. Let this be denominated as the disec (combination of the words "dimensionless" and "second".) In this paper, the unit of the disec is taken as the ratio of the duration of time for a sound wave to travel the length of the beam to the duration of a second. The dimensionless frequency is then expressed as radians per disec or cycles per disec. The dimensionless period is expressed in disecs per cycles. If Ω is the dimensionless frequency in radians per space disec, φ the dimensionless frequency in cycles per disec, and Υ the dimensionless period in disecs/cycle, these three quantities satisfy the relations

$$\phi = \frac{1}{\Upsilon}$$

$$\Omega = 2\pi\phi = \frac{2\pi}{\Upsilon}$$

Ω, φ, and Υ for the beams of Table I are shown in Table II. These numbers are easily interpreted. Beam I vibrates through 0.0409 radians or 0.00650 cycles in the time required for a sound wave to travel its length. Conversely, while the beam was vibrating through one cycle a sound wave would travel its length 154 times.

TABLE II.

Beam No.	rad/disec	cycles/disec	disec/cycle
1	0.0409	0.00650	154
3	0.0410	0.00653	153
4	0.0404	0.00644	155
11	0.0410	0.00653	153
12	0.0404	0.00644	155
13	0.0407	0.00649	154
15	0.0403	0.00642	156
16	0.0404	0.00644	155
21	0.0405	0.00645	155

The maximum strains developed in each beam as measured in Test I are plotted against dimensionless time in Fig. 17. This plot discloses many points of interest.

In the first place the agreement amongst the curves is noteworthy. The agreement between strains as predicted from any one beam as prototype is well within the $\pm$ 10 percent predicted in the Introduction. In the first few disecs when the strain is highest the strain values vary only from 315 μ in/in. to 324 μ in./in. - a variation of $\pm$ 1.41 percent of the mean value. For later times, the variation increases. Thus at 5400 disecs (approximately 35 cycles of stress) the variation is from 177 μ in/in. to 215 μ in/in. This amounts to $\pm$9.68 percent of the mean value. At 10,000 disecs (approximately 70 cycles of stress) the variation is from 139 μ in/in. to 165 μ in/in. This is $\pm$ 8.57 percent of the mean value.

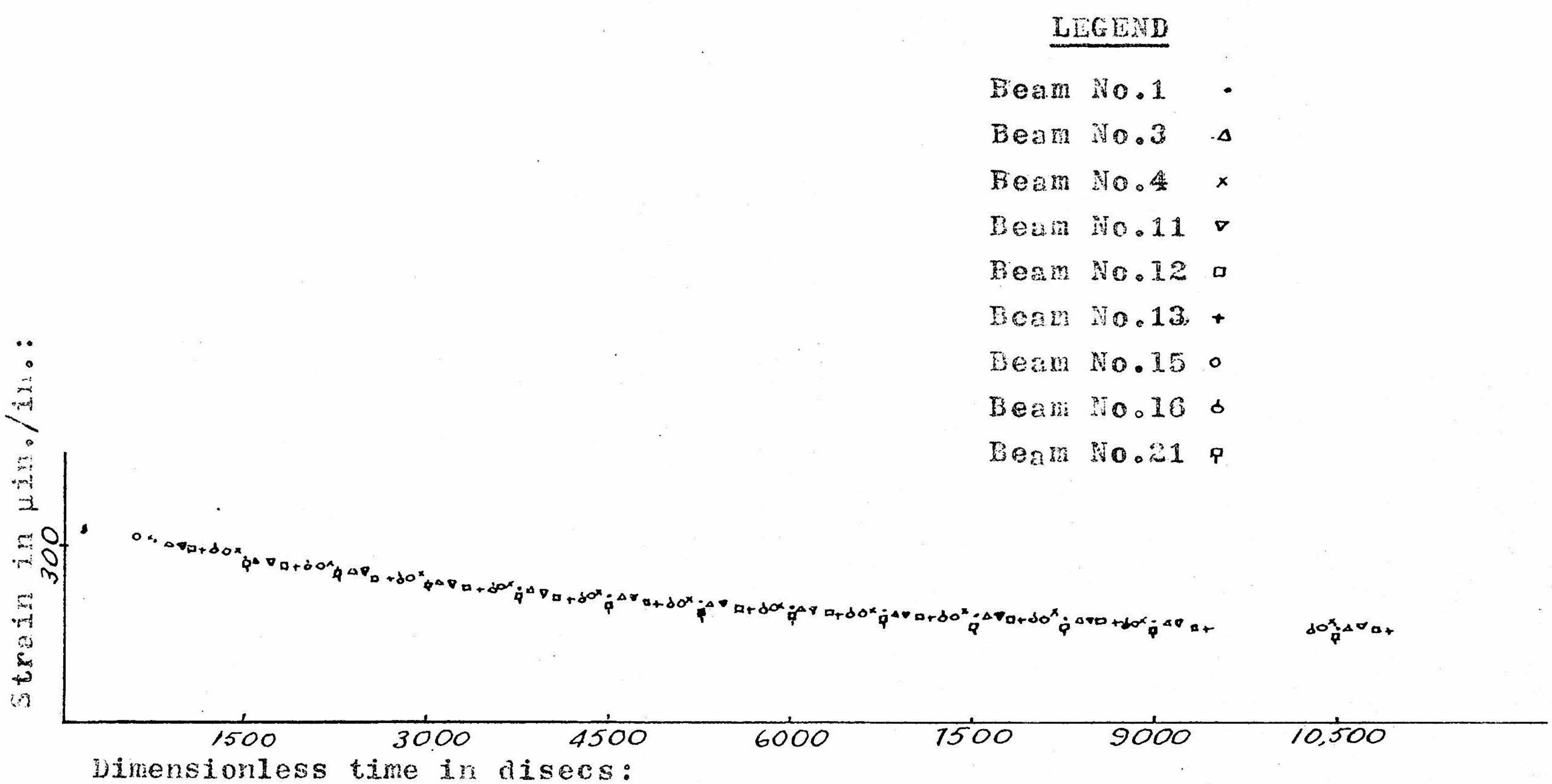

Fig. 17. Strain-decay curves for ten modeled beams.

In all the curves the strain at the end of the first cycle was greater than the statical strain by 5 percent to 8 percent of the statical strain. This apparent paradox can be explained on the grounds that because of the larger number of cycles in unit time the higher modes damp out more rapidly than does the fundamental. This fact combined with the fact that the curvature of the beam when it is vibrating freely in its fundamental mode differs widely from its curvature when it is subjected to a statical deflection gives rise to higher vibrating strains than the statical strains from which they spring.

In order to illustrate this point, let us consider a fixed-free beam. Let the beam be statically deflected by a concentrated load P applied at the free end. Let E be Young's Modulus for the materials, I the cross-sectional moment of inertia, and L the length. Let us assume that the deflection is small enough that the curvature can be taken equal to $\frac{d^2y}{dx^2}$. We have then that the maximum strain at any section of the beam is proportional to the curvature at that section. For the statical deflection the deflection curve is

(61) $$y = -\frac{Px^2}{6EI}(3L-x)$$

and the maximum curvature is

(62) $$\left.\frac{d^2y}{dx^2}\right|_{x=0} = -\frac{PL}{EI}$$

If the load is suddenly released, the beam will vibrate in an infinity of modes, each mode being one of the eigen-functions. The higher modes will damp out rapidly, leaving only the fundamental mode. By this time the beam no longer has the cubical parabolic shape given by Eq. (61) but has the shape of the first eigen-function.

In an effort to appraise the curvature in this latter event, let us determine the curvature at the root of the beam for the first mode at time t = 0. To this end we write the eigen-function expansion for the statical deflection curve

(63) $$-\frac{Px^2}{6EI}(3L-x) = \sum_{i=1}^{\infty} \frac{2P}{p_i^4 LEI} X_i$$

where

$$X_i = \cos p_i x - \cosh p_i x - \frac{\cos p_i L + \cosh p_i L}{\sin p_i L + \sinh p_i L}(\sin p_i x - \sinh p_i x)$$

Whence

(64) $$\left.\frac{d^2y}{dx^2}\right|_{x=0} = -\frac{PL}{EI} = \sum_{i=1}^{\infty} \frac{-4P}{p_i^2 LEI}$$

where the second and third members are obtained by differentiating the LHS and RHS of Eq. (63) resp.

For the first mode, p = 1.875/L. Hence the first term of the summation on the right has the value 1.137 PL/EI. Comparison of this value with Eq. (62) shows that the curvature at the root in the first mode exceeds the statical curvature by 13.7 percent of the statical curvature. The strains will be in the same ratio. This represents the maximum possible over-strain, actually, the higher modes will not necessarily be damped out during the first cycle but might possibly endure into the second cycle depending on the magnitude of the damping in the system. During this time there will be some damping of the first mode, too. The result is that the dynamic strain rarely exceeds 110 percent of the static strain.

In similar fashion other types of beams can be investigated. For example, for the fixed-free beam with uniform load the dynamic strain at mid-span due to a sudden removal of the load is 121.0 percent of the statical strain at this point. In a beam of uniform section the statical strain at mid-span is half the maximum strain so this over-strain of 121.0 percent is not serious. The results cannot, of course, be applied directly to a beam of varying cross section, but in such a case similar investigations should be carried out.

Again, upon sudden removal of the load a hinged-hinged beam with concentrated load at mid-span will show at a point 1/10 the length of beam from the end an over-strain of 126.0 percent of the statical strain. Should an over-strain of this magnitude develop at a point in a beam of constant strength the results could be disastrous. An investigation along those lines should be undertaken for all such beams.

The dimensions of the beams which were tested were carefully chosen in such a fashion that the relative importance of structural damping and internal damping would be revealed. Thus beams 1, 3,4, 11, 13, 16 and 21 all were 1 in. in width. They all presented the same area to the vise. All were tightened to the same bolting load. All were subjected to the same strain at the root. From the agreement of the curves of Fig. 17 it follows that the same percentage energy was dissipated by each beam in corresponding cycles. Since all beams had different frequencies, and since internal damping is independent of frequency, the conclusion is reached that the structural damping is either independent of frequency or is sufficiently small that its effects are overshadowed by those of internal damping. To resolve this alternative beams 12 and 17 were included. Beam 12 was 1-1/2 in. wide and was proportioned according to the modeling parameters. Beam 17 was also 1-1/2 in. wide but was not proportioned to satisfy the requirements for modeling of internal damping. In fact, by being 1/2 in. wider than Beam 16 but of the same thickness and length it was known to have greater internal damping than Beam 16. However, it presented the same area to the vise as did Beam 12 and the same strain was developed at its root. The strain decay curves for these beams are shown in Fig. 18. The only variable between Beams 12 and 17 which might influence the structural damping is the frequency. But it has already been concluded from Beams 1, 3, 4, 11, 13, 16 and 21 that the structural damping is independent of the frequency or else is small enough that its effects are overshadowed by the internal damping. Hence, the difference between the two curves of Fig. 18 can only be accounted for by the conclusion that the effect of structural damping is small in comparison with the effect of internal damping. In other words, the agreement amongst the curves of Fig. 17

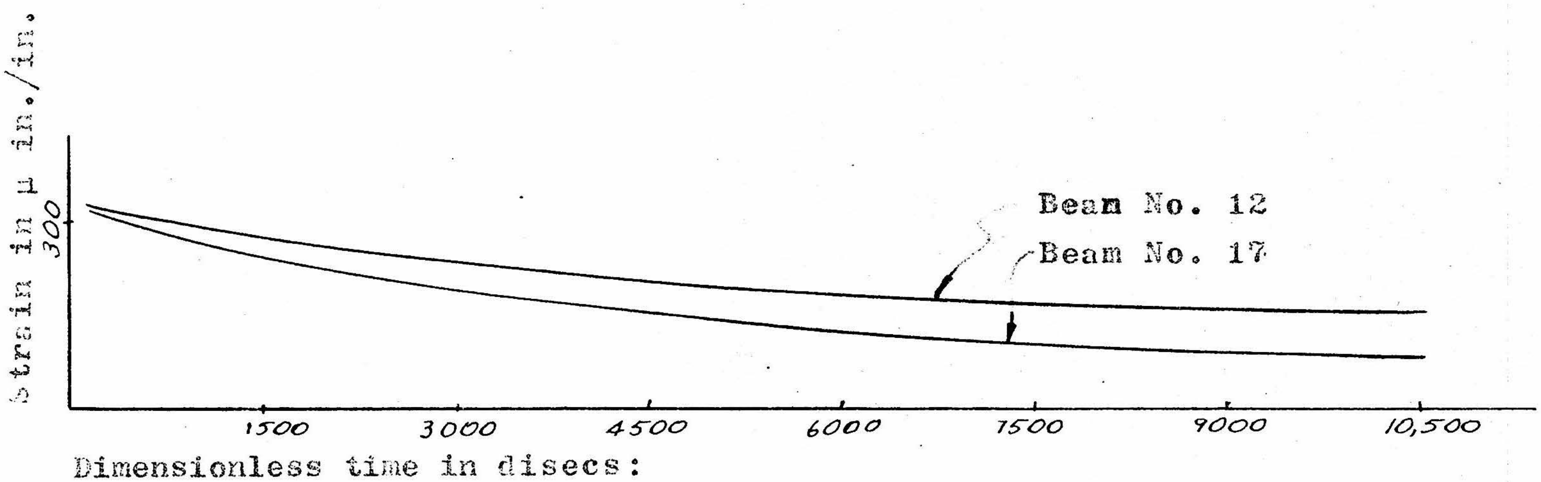

Fig. 18. These two beams were subjected to the same external damping. The effect of their different internal damping shows clearly in the difference between the two curves

is due to a correct modeling of internal damping, not to a constant percentage energy loss through structural damping.

The other tests, namely Test 1(f), seeking to evaluate the effects of structural damping, only served to strengthen this conclusion. When the vise was supported by a long fine wire the over-strain at the end of the first cycle was decreased and subsequent strains were increased. For Beam No. 31, the opposite situation was true. The two curves for this latter beam are plotted in Fig. 19.

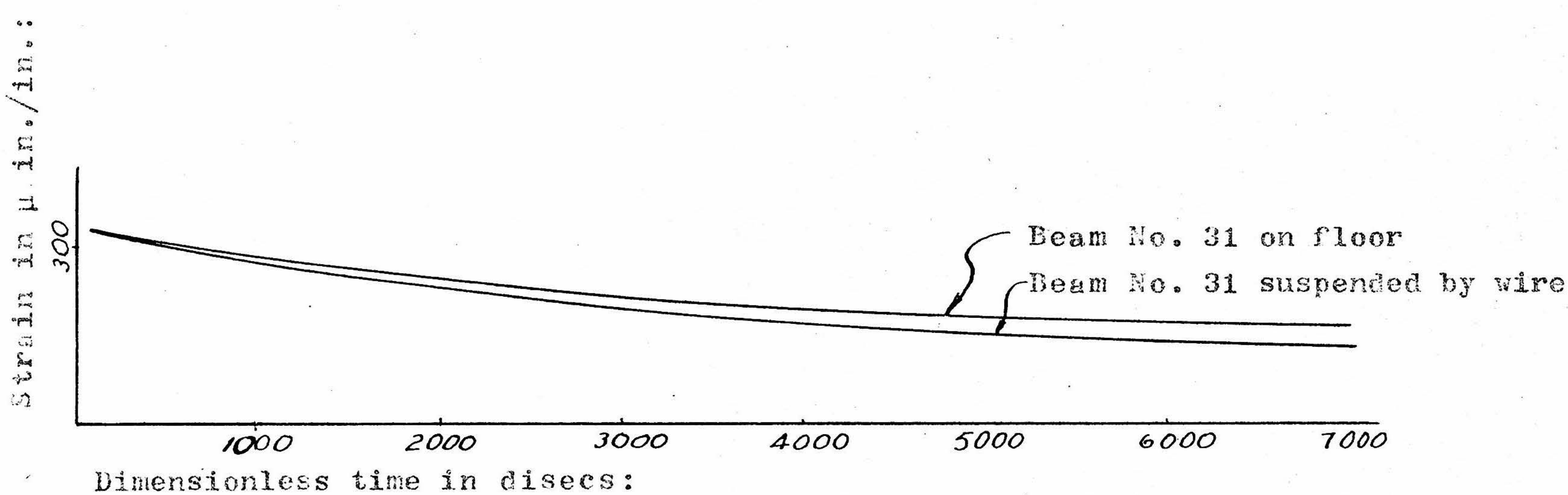

Fig. 19. The effect of changing the external damping is shown in the difference between the two curves.

THE DROP TESTS:

In Fig. 20 is shown a tracing of the acceleration and strain vs. time curves for the series of drop tests outlined in Chapter II. The uniformity of results was anticipated from previous investigations of the accelerations undergone by a drop table while being stopped by a short lead column. The data as gathered show the strain as ordinate to different scales. This is due to the different sensitivities of the various galvanometer elements. The magnitudes of these strains can be readily compared however. For Drops Nos. 1, 3, and 5, the acceleration was reasonably uniform. In Drop No. 1 the maximum strain indicated for Beam No. 22 by channel II is the same as that indicated by this same channel for Beam No. 23 in Drop No. 3. Hence we conclude that for the same acceleration, the maximum strains in Beams Nos. 22 and 23 are the same within satisfactory limits. In the same manner, a comparison of the records of Channel III of Drops Nos. 3 and 5 allows us to conclude that the maximum strains developed in Beams Nos. 23 and 24 are reasonably the same. The curves for Drop No. 6 are plotted to correct dimensionless scales in Fig. 21. These curves all show the same maximum strain. Actually the sensitivity of the instrumentation is such that these three maxima might vary by as much as $\pm$ 5 percent. This is well within the limits of acceptability set forth in the Introduction.

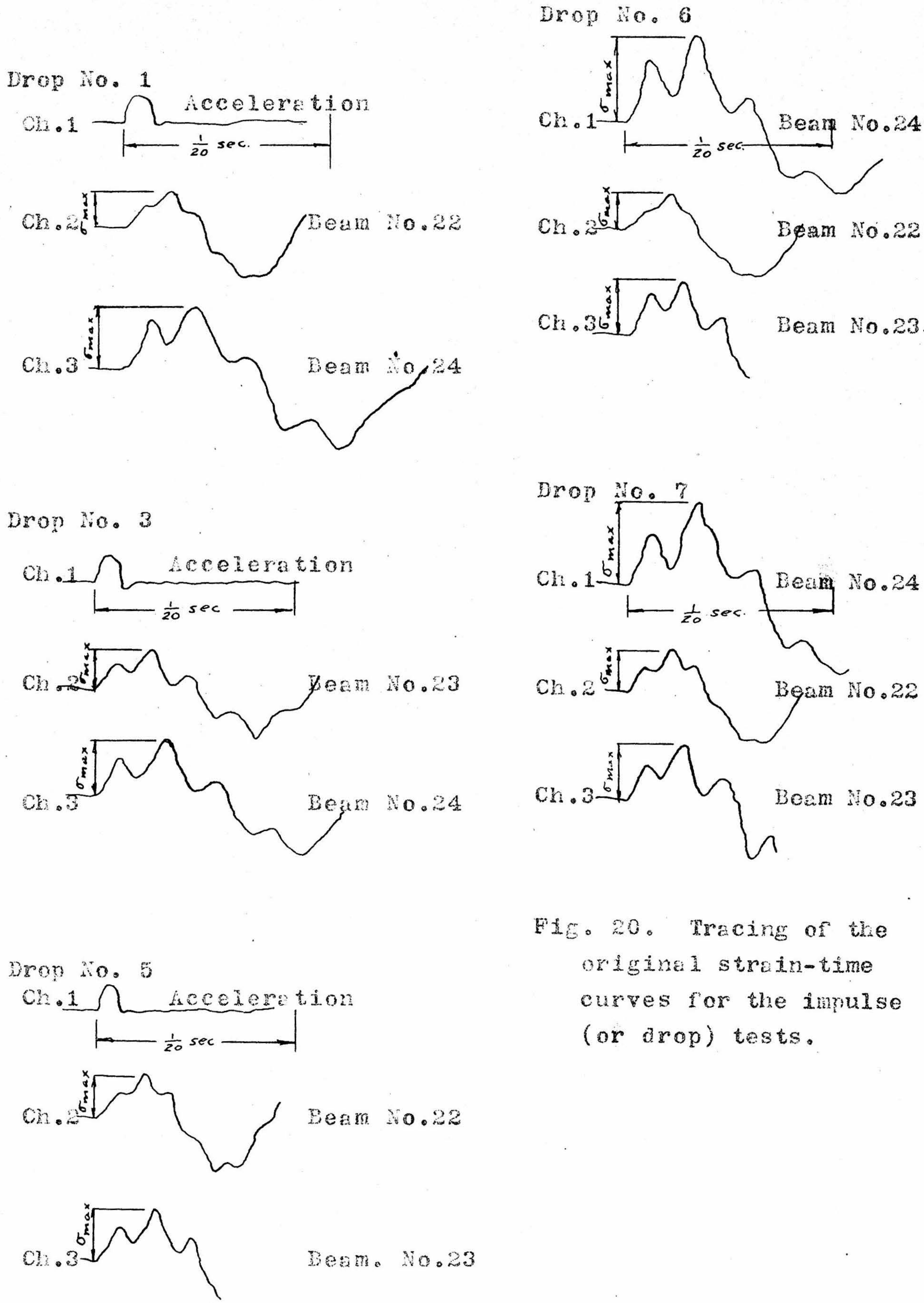

Fig. 20. Tracing of the original strain-time curves for the impulse (or drop) tests.

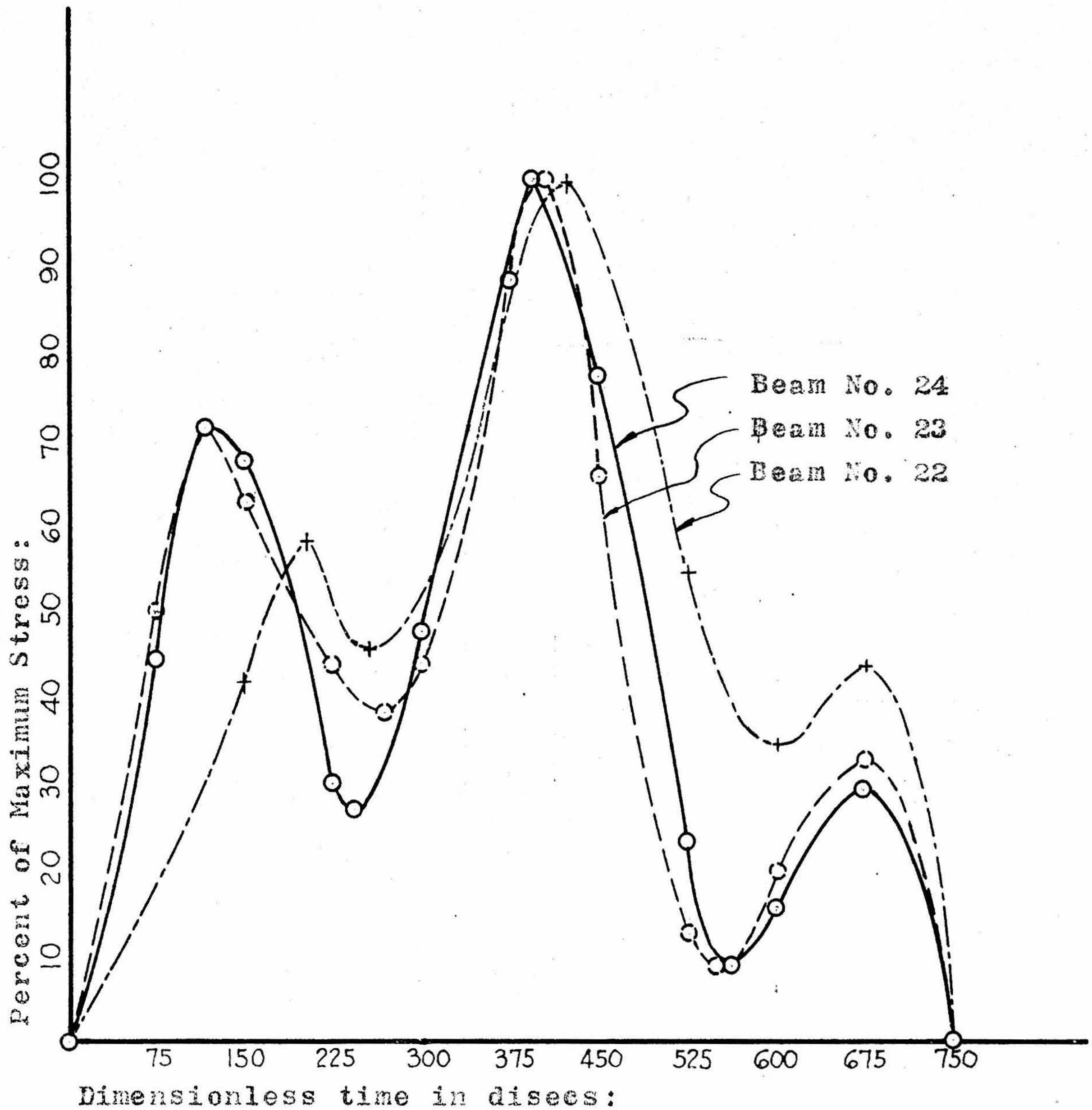

Fig. 21. Dynamic Response of Three Beams Whose Roots Are Subjected to the Same Acceleration. (Plotted from the Original Data by Proportional Dividers.)

The agreement in shape of the strain vs. time curves which appears in Fig. 21 deserves further consideration. The theory developed in Chapter II showed that the strains should be the same, but this theory was based on the assumption that there was no damping. It is generally believed that the damping in such a case as this would play so important a role as to render valueless an analysis ignoring damping. This belief can be reconciled with these results through the realization that the acceleration of the roots of these beams was of very short duration as indicated in Table III.

The damping is an energy dissipation which does not occur until the material has reached maximum strain and the strain is being reversed. As a result we would not anticipate the effect of damping to make itself felt in any mode until after the first quarter cycle of that mode. For the three beams under consideration the acceleration has ceased before the first eighth of a cycle of the fundamental mode and the three beams are then vibrating in essentially the same fashion as the beams of Test I. The damping in the first mode will be essentially the same for all beams in view of the results of the strain decay tests.

For the higher modes the acceleration has longer relative duration as noted in Table III. The second mode whose period is approximately one-seventh that of the first mode is generated by an acceleration whose duration is between 50 and 75 percent (approximately) of the period of the mode.

Some reduction due to damping of the strain in this mode should then be anticipated. This decrease in strain amplitude becomes noticeable after the first cycle of this mode. Likewise, for the three modes, whose period is approximately one-twentieth of the period of the fundamental mode, the acceleration endures for 1 to 2 complete cycles. Throughout all of this the acceleration against time curve can be reasonably approximated by ~~a step function~~ an impulse. Consequently, we would not expect the damping to make itself felt in the higher mode until after its second or third cycle. Moreover, the contribution to the total strain of these higher modes is small. Thus, though the damping may appreciably influence the magnitude of strain due to each mode the net result is that the strains are adequately modeled in the three beams.

Beam No.	Duration of Acceleration (disecs)	Period of 1st Mode (disecs)	Duration of acceleration (% of 1st Mode)
22	93.5	744	12.6
23	62.5	744	8.40
24	46.8	744	6.29

Beam No.	Duration of Acceleration (disecs)	Period of 2nd Mode (disecs)	Duration of Acceleration (% of 2nd Mode)
22	93.5	119	78.6
23	62.5	119	52.3
24	46.8	119	49.4

Beam No.	Duration of Acceleration (disecs)	Period of 3rd Mode (disecs)	Duration of Acceleration (% of 3rd Mode)
22	93.5	42.4	220.3
23	62.5	42.4	147.5
24	46.8	42.4	110.3

TABLE III.

THE FORCED VIBRATION TESTS:

In these tests, beams Nos. 32 to 37 were subjected to a scaled acceleration by being mounted on a shaking table. The beams were vibrated at frequencies between 50 percent and 90 percent of resonance. The theory developed in Chapter I indicates that for adequate modeling of this type the amplitude of sinusoidal vibration of the shaking table must be proportional to the length of the beam.

In an effort to evaluate the effect of internal damping on the strains developed two beams were used in each run, one being a beam which was thoroughly and carefully annealed, the other being of cold rolled stock. Both the beams satisfied the SAE 1025 specification.

Moreover, to have an actual indication of the effect of change of internal damping on the amplitude, one of the tests was made over a considerable period of time so that the change in internal damping of the annealed beam could make itself felt.

It was observed that in a period covering some 1,100,000 cycles there was a change in the internal damping of the annealed beams in that the strains developed in these beams varied by approximately 10 percent. The results of the test however show that in this range of frequencies the effect of a variation of internal damping is very small and the strains developed in the beams were within the acceptable limit of accuracy. The results are tabulated in Table IV for the long duration runs.

TABLE IV.

Beam No.	Frequency (r.p.m.)	Amplitude of Vibration of shaking table (inches)	Strain (μ in./in.)
32	1750	0.041	178-185
35	1750	0.041	185-200
33	2335	0.031	184-208
36	2335	0.031	190-205
34	3500	0.020	186-208
37	3500	0.020	195-210

The conclusion to be drawn is that for forced vibrations below resonance, the effect of internal damping can be modeled.

For forced vibrations at resonance, the situation is not so clear cut. The strains in Beams Nos. 32 and 35 were respectively 1000 μ in./in. and 980 μ in./in. For Beams Nos. 33 and 36 the strains were 1000 μ in./in. and 990 μ in./in. Thus it appears that the difference in internal damping, if any difference exists, between the annealed beams and the cold rolled beams has little effect on the strains developed. However, the smaller beams required an amplitude of vibration of their roots of only 27.8 percent of that required by the larger beams to develop the same strain. Were the amplitude of strain at resonance governed by internal damping only, then the analysis of Chapter I would indicate that the required amplitude of vibration of the roots of Beams Nos. 33 and 36 would be three-fourths that required for Beams Nos. 32 and 35. The conclusion is then reached that at resonance internal damping is not the controlling factor. This agrees with experience. For example, Hamstock and Murray[16] in reporting tests of internal damping point out that in most systems the magnitude of the strains developed at resonance depends on the external damping rather than on the internal damping.

SUMMARY OF TEST RESULTS:

The results of these tests can be summarized as follows: The analysis indicates that in those applications where internal damping can be neglected, modeling for stress similitude can be attained if the dimensionless radius of gyration is the same for prototype and model. This conclusion was substantiated by the free vibration test and by the drop test. In each of these tests the strain vs. dimensionless time curves were essentially the same for prototype and model.

For those applications wherein the internal damping is of importance, the analysis shows that geometric similarity between prototype and model is necessary for adequate modeling. The free vibration test of Beam No. 17 and the forced vibration tests of Beams Nos. 32-27 showed this to be true. Moreover, the long-time forced vibration test showed that the effect of a change in the internal damping of the beam on the strains developed is small. Thus, for example, even though the magnitude of the internal damping for Beam 32 in the annealed state was different from that for Beam 35, the strains developed in the two when their roots were subjected to the same acceleration were in acceptably close agreement.

CHAPTER IV.

In this chapter an extension of the analyses of Chapter I is made to the question of vibration of plates and frames.

PLATES:

The equation of motion for a vibrating plate is well known[17]. It is

$$\frac{Eh^3}{3\rho(1-\mu^2)}\nabla^4 w = Z - \ddot{w} \tag{65}$$

where E is Young's Modulus

ρ is the density of the material

h is the half thickness of the plate

w is the displacement of the middle surface from its unstrained position which coincides with the x-y plane

$Z = Q/2\rho h$ where Q is the transverse force acting on a surface element

The bending moments M_x and M_y in the x and y directions are given by the expressions

$$M_x = -\frac{Eh^3}{3(1-\mu^2)}\left(\frac{\partial^2 w}{\partial x^2} + \mu\frac{\partial^2 w}{\partial y^2}\right) \tag{66}$$

and

$$M_y = -\frac{Eh^3}{3(1-\mu^2)}\left(\frac{\partial^2 w}{\partial y^2} + \mu\frac{\partial^2 w}{\partial x^2}\right) \tag{67}$$

Finally the maximum stresses $\sigma_{x_{max}}$ and $\sigma_{y_{max}}$ in the x- and y- directions are given by

$$\sigma_{x_{max}} = \frac{3M_x}{2h^2} \tag{68}$$

and

(69) $$\sigma_{y_{max}} = \frac{3M_y}{2h^2}$$

while the maximum shearing stress

(70) $$\tau_{max} = \frac{3(M_x - M_y)}{4h^2}$$

or

(71) τ_{max} = the larger of Eq.(68)or (69)

depending on whether the stresses of Eqs. (68) and (69) are of opposite or like sign.

Define

$x = L\xi$ where L is a characteristic length

$y = L\eta$

$w = L\zeta$

$h = L\delta$

$a^2 = E/\rho$

$t = L\tau/a$

$b = Q/E$

With the foregoing definitions, we easily find that

(72) $$\frac{\partial^{m+n} w}{\partial x^m \partial y^n} = L^{1-m-n} \frac{\partial^{m+n}\zeta}{\partial \xi^m \partial \eta^n}$$

and

(73) $$\frac{\partial^n w}{\partial t^n} = a^n L^{1-n} \frac{\partial^n \zeta}{\partial \tau^n} \qquad (m, n, = 1, 2, \cdots)$$

Making the substitutions (72) and (73) in Eq. (66) leads to the dimensionless form of the equation of motion:

~~(74)~~ $$\cancel{\frac{\delta^2}{3(1-\mu^2)} \nabla'^4 \zeta - \frac{b}{2\delta} + \frac{\partial^2 \zeta}{\partial \tau^2} = 0}$$

~~where ∇' has been written to call attention to the fact that~~

(74)
$$\frac{\delta^2}{3(1-\mu^2)} \nabla'^4 \zeta - \frac{b}{2\delta} + \frac{\partial^2 \zeta}{\partial \tau^2} = 0$$

where ∇' has been written to call attention to the fact that these differentiations are with respect to ξ and η

If we now define dimensionless stresses by the relationship: dimensionless stress, Σ , = ratio of actual stress to Young's Modulus, Eqs. (68) and (69), and in consequence Eqs. (72) and (73), can be rendered in the dimensionless forms

(75)
$$\Sigma_{x_{max}} = -\frac{\delta}{3(1-\mu^2)} \left(\frac{\partial^2 \zeta}{\partial \xi^2} + \mu \frac{\partial^2 \zeta}{\partial \eta^2} \right)$$

(76)
$$\Sigma_{y_{max}} = -\frac{\delta}{3(1-\mu^2)} \left(\frac{\partial^2 \zeta}{\partial \eta^2} + \mu \frac{\partial^2 \zeta}{\partial \xi^2} \right)$$

The boundary conditions when stated dimensionlessly become:

A) For a built-in edge parallel with the x-axis and at y=c

(77)
$$\zeta \Big|_{\eta = \frac{c}{L}} = 0 \qquad \frac{\partial \zeta}{\partial \eta} \Big|_{\eta = \frac{c}{L}} = 0$$

B) For a simply supported edge parallel with the x-axis and at y = c

(78)
$$\zeta \Big|_{\eta = \frac{c}{L}} = 0 \qquad \frac{\partial^2 \zeta}{\partial \eta^2} \Big|_{\eta = \frac{c}{L}} = 0$$

(C) For a free edge parallel with the x-axis and at y = c

(79)
$$\begin{cases} \left. \dfrac{\partial^3 \zeta}{\partial \eta^3} + (2-\mu) \dfrac{\partial^3 \zeta}{\partial \xi^2 \partial \eta} \right|_{\eta = \frac{c}{L}} = 0 \\[2ex] \left. \dfrac{\partial^2 \zeta}{\partial \eta^2} + \mu \dfrac{\partial^2 \zeta}{\partial \xi^2} \right|_{\eta = \frac{c}{L}} = 0 \end{cases}$$

Conditions on edges parallel with the y-axis can be obtained from Eqs. (77) - (79) by permuting ξ and η. For plates of shapes other than rectangular the more general boundary conditions given by Rayleigh, pg. 357 should be used.

From the foregoing discussion, we conclude that the vibration of plates can be successfully modeled in accordance with the following principles:

I. If the prototype has simply supported or rigidly built in edges, the model may be of any material so long as the thickness and the applied load are selected in such manner that $\delta^2/[3(1-\mu^2)]$ and $b/(2\delta)$ are the same for prototype and model.

II. If the prototype has a free edge, the model must be of a material having the same Poisson's ratio as the prototype. This conclusion follows from the presence of μ in the boundary conditions, Eqs. (77) and (78).

Consider now a flat plate with no load (Q=0) and choose the x-y plane to coincide with its unstrained middle surface. Let the x-y plane be subjected to an acceleration f(t) in the z direction. We shall discuss the subsequent vibratory motion of the plate. Let X, Y, and Z be a set of stationary axes, the Z and z axes coinciding, and the x- and y- axes remaining parallel to the X- and Y- axes. Let $Z_0 = Z_0(t)$ be the coordinate of the moving origin, W, the displacement of any point on the middle surface of the plate referred to the stationary axes and w the displacement of the same point referred to the moving axes. Then

(80) $$W = Z_o + w$$

Equation (65) becomes, upon substitution of Eq. (80)

(81) $$\frac{Eh^3}{3\rho(1-\mu^2)} \nabla^4 w + \ddot{Z}_o + \ddot{w} = 0$$

since Z_0 is independent of X and Y. The differentiations involved in ∇^4 can be taken either with respect to X and Y or with respect to x and y since X = x and Y = y. Comparison of Eq. (80) with Eq. (65) reveals that a uniformly distributed arbitrary forcing function Q = Q(t) acting on the plate can be studied by subjecting the middle surface of the plate to an arbitrary acceleration $Z_0 = Z_0(t)$, the relationship being that

(82) $$Z_o(t) = -\frac{1}{2\rho h} Q(t)$$

Equation (82) can be put into dimensionless form by using our usual substitutions. Thus

(83) $$Z_o\left(\frac{L\tau}{a}\right) = -\frac{1}{2\rho L\delta} Q\left(\frac{L\tau}{a}\right)$$

It appears then that the method of analysis developed and tested for beams can readily be extended to the modeling of plates.

FRAMES:

In order to investigate the possibility of using the modeling parameters already developed for beams and plates as the modeling parameters for frames, let us consider the differential equations of motion for the frame shown in Fig. 22 which is hinged at points A and D and has rigid right angle joints at B and C. The vertical members of the frame have area A; and sectional moment of inertia I_1, while the horizontal member has the values A_2 and I_2 respectively. The material of the three bars is the same and is of specific weight γ.

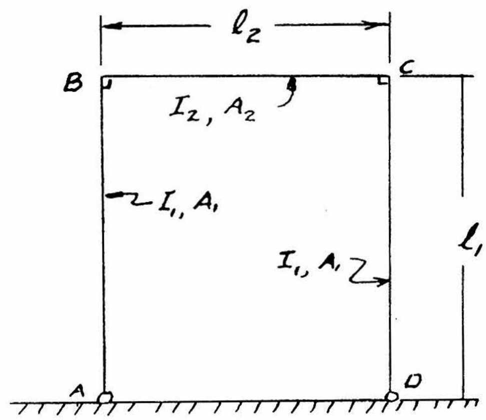

Fig. 22

The differential equations of motion can best be established by the application of Hamilton's Principle.

In order to write the expressions for the strain energy and kinetic energy of the system choose x-y axes with origin at A and x-axis along AB. Choose u-v axes with origin at B and u-axis along BC. If we consider only small vibrations, then the strain energy due to direct stress is negligible in comparison with the strain energy due to bending, and we can write:

$$(84) \qquad V = 2\int_0^{l_1} \frac{EI_1}{2}\left(\frac{d^2y}{dx^2}\right)^2 dx + \int_0^{l_2} \frac{EI_2}{2}\left(\frac{d^2v}{du^2}\right)^2 du$$

In computing the kinetic energy we realize that the bars AB and DC are undergoing bending vibrations only, whereas the bar BC in addition to its bending vibration is possibly subjected to a translatory vibration in the direction BC. The kinetic energy of this latter motion is not always negligible. It can be expressed as $\frac{1}{2}\frac{A_2 l_2 \gamma}{g}\left(\dot{y}\big|_{x=l_1}\right)^2$ where the notation $\dot{y}\big|_{x=l_1}$ signifies the velocity of the upper end of the bar AB. Other types of energy, e.g. strain energy due to direct stress, kinetic energy due to rotary inertia, will be ignored. The expression for the kinetic energy is

$$(85) \qquad T = 2\int_0^{l_1} \frac{A_1\gamma}{2g}\dot{y}^2 dx + \int_0^{l_2} \frac{A_2\gamma}{2g}\dot{v}^2 du + \frac{1}{2}\frac{A_2 l_2 \gamma}{g}\left(\dot{y}\big|_{x=l_1}\right)^2$$

We have then

$$(86) \qquad \delta V = 2EI_1\left\{\frac{d^2y}{dx^2}\,\delta\frac{dy}{dx} - \frac{d^3y}{dx^3}\,\delta y + \int_0^{l_1}\frac{d^4y}{dx^4}\,\delta y\,dx\right\}$$
$$+ EI_2\left\{\frac{d^2v}{du^2}\,\delta\frac{dv}{du} - \frac{d^3v}{du}\,\delta v + \int_0^{l_1}\frac{d^4v}{du^2}\,\delta v\,du\right\}$$

where the terms free from the integral sign are to be taken between the limits. We also find that

$$(87) \qquad \delta\int_{t_0}^{t_1} T\,dt = \int_{t_0}^{t_1}\left\{-\frac{2A_1\gamma}{g}\int_0^{l_1}\frac{d^2y}{dt^2}\,\delta y\,dx - \frac{A_2\gamma}{g}\int_0^{l_2}\frac{d^2v}{dt^2}\,\delta v\,du\right.$$
$$\left. - \frac{A_2 l_2\gamma}{g}\,\frac{d^2y}{dt^2}\bigg|_{x=l_1}\,\delta y\bigg|_{x=l_1}\right\} dt.$$

The variational equation of motion is then

$$(88)\qquad \int_0^{l_1}\left(2EI_1\frac{\partial^4 y}{\partial x^4}+\frac{2A_1\gamma}{g}\frac{\partial^2 y}{\partial t^2}\right)\delta y\,dx+\int_0^{l_2}\left(EI_2\frac{\partial^4 v}{\partial u^4}+\frac{A_2\gamma}{g}\frac{\partial^2 v}{\partial t^2}\right)\delta v\,du$$

$$+2EI_1\left(\frac{\partial^2 y}{\partial x^2}\delta\frac{\partial y}{\partial x}-\frac{\partial^3 y}{\partial x^3}\delta y\right)\Bigg|_0^{l_1}+EI_2\left(\frac{\partial^2 v}{\partial u^2}\delta\frac{\partial v}{\partial u}-\frac{\partial^3 v}{\partial u^3}\delta v\right)\Bigg|_0^{l_2}$$

$$+\frac{A_2 l_2\gamma}{g}\frac{\partial^2 y}{\partial t^2}\Bigg|_{x=l_1}\delta y\Bigg|_{x=l_1}=0.$$

From Eq. (88) we conclude that the differential equations of motion for the frame are

$$(89)\qquad EI_1\frac{\partial^4 y}{\partial x^4}+\frac{A_1\gamma}{g}\frac{\partial^2 y}{\partial t^2}=0$$

and

$$(90)\qquad EI_2\frac{\partial^4 v}{\partial u^4}+\frac{A_2\gamma}{g}\frac{\partial^2 v}{\partial t^2}=0.$$

while the boundary conditions are those imposed by the evanescence of the integrated terms in Eq. (88).

The implications of Eqs. (88), (89), and (90) are many and important:

1. The method by which these equations were obtained is general and can be extended readily to more complicated frames. It follows that modeling methods based on this analysis will have the same generality--that such modeling methods will also be readily extended to more complicated frames.

2. It is possible to predict the natural frequency of frames without damping by a mathematical method analogous to that used for bars.

3. As stated in (2) above, it is possible to predict the natural frequency of frames without damping. The numerical work involved in this determination follows the same pattern as that for bars but is considerably more onerous. It would be desirable to reduce this work to tabulated form for the benefit of the profession. For illustration, the determination of the frequencies of the symmetrical modes of vibration of the frame shown in Fig. 22 is outlined in Appendix V.

4. In spite of the greater numerical complexities, the theoretical treatment of the vibration of frames is now placed on as sound a logical basis as underlies the treatment of the vibration of bars. Moreover, the implication of Eqs. (88) and (89) that each member of a vibrating frame executes its transverse vibrations in modes having the same shape as the modes in which it vibrates as a beam allows us to deduce that the conclusions already reached in the question of modeling of beams for dynamic stress similitude can be applied immediately to the modeling of frames.

BIBLIOGRAPHY

(1) Timoshenko, S., "Strength of Materials", D. Van Nostrand, N. Y. (1940)

(2) Timoshenko, S., "Theory of Elasticity", McGraw-Hill, N.Y. (1934)

(3) Norris, Chas. H., "Model Analysis of Structures", Proc. Soc. for Exp. Stress Anal., Vol. I, No. 2, pg. 19, (1944)

(4) Sezawa, K., "On the Decay of Waves in Visco-Elastic Solid Bodies", Tokyo Imperial Univ., Vol. III, (Sept. 1927)

(5) Mindlin, Stubner, and Cooper, "Response of Damped Elastic Systems to Transient Disturbances", Proc. Soc. for Exp. Stress Anal., Vol. V, No. 2, pg. 69 (1948)

(6) Thompson, F.C., "Damping Capacity", British Non-Ferrous Metals Research Ass'n. London, (1944)

(7) Föppl, O., "The Practical Importance of the Damping Capacity of Metals, Especially Steels", Wöhler Inst., (1936)

(8) Lazan, "Some Mechanical Properties of Plastics and Metals Under Sustained Vibrations", Trans., ASME Vol. 65, pg. 87, (Feb. 1943)

(9) Kimball and Lovell, "Internal Friction in Solids", Phy. Review, Vol. 30, pg. 948, (Dec. 1927)

(10) Schabtach and Fehr, "Measurement of Damping of Engineering Materials During Flexural Vibrations at Elevated Temperatures", Jour. of App. Mech., Vol. 66, pg. A-86 (June 1944)

(11) Jacobsen, L.S., "Steady Forced Vibrations as Influenced by Damping", Trans., ASME, Vol. 52(1) pg. 169 (1930)

(12) Myklestad, "Vibration Analysis", McGraw-Hill, (1944)

(13) Kimball, "Vibration Problems", Jour. of App. Mech., Vol. 63, pg. A-37, (March 1941)

(14) Robertson and Yorgiadis, "Internal Friction in Engineering Materials", Jour. of App. Mech., Vol. 68, pg. A-173, (Sept. 1946)

(15) Timoshenko, S., "Vibration Problems in Engineering" D. Van Nostrand, N. Y. (1937)

(16) Hamstock and Murray, "Damping Capacity and Fatigue of Metals", Engineering, Vol. 161, pg. 358, (April 1946)

(17) Rayleigh, "Theory of Sound". Dover, N.Y. (1945)

(18) Den Hartog, "Mechanical Vibrations", McGraw-Hill, N. Y. (1947)

(19) Prescott, John, "Applied Elasticity". Dover, N.Y (1946)

APPENDIX I.

It became evident early in the course of this investigation that a uniform choice of form of solution of the dimensionless equation of motion for a freely vibrating beam was desirable. The usual reference works ([15]), ([17])([18]) ([19]), all give the eigen-functions in different form. The forms which are listed below seem to be the most useful. In Appendix II it is shown that these functions are normalized.

The dimensionless equation of motion for a freely vibrating beam is

$$\eta = \sum_{i=1}^{\infty} \Xi_i(\xi)(A\cos\Omega_i\tau + B\sin\Omega_i\tau)$$

For convenience of reference the functions $\Xi_i(\xi)$, the dimensionless frequency equation, its first five roots and the first five dimensionless natural frequencies, Ω_i are listed for each type of beam. h is the dimensionless radius of gyration. To obtain the actual natural frequency, ω_i, of a beam it is only necessary to multiply its dimensionless natural frequency, Ω_i, by the ratio of the speed of sound, a, in the material to the length, L, of the bar, thus

$$\omega_i = \frac{\Omega_i a}{L}$$

<u>For the hinged-hinged beam:</u>

$$\Xi_i(\xi) = \sqrt{2}\sin p_i\xi$$

$$\sin p_i = 0$$

p_1	p_2	p_3	p_4	p_5
π	2π	3π	4π	5π

Ω_1	Ω_2	Ω_3	Ω_4	Ω_5
9.870κ	39.478κ	88.826κ	157.01κ	246.75κ

For the free-free beam:

$$\Xi_i(\xi) = \cos p_i\xi + \cosh p_i\xi + \frac{\sin p_i + \sinh p_i}{\cos p_i - \cosh p_i}(\sin p_i\xi + \sinh p_i\xi)$$

$$\cos p_i \cosh p_i = -1$$

p_1	p_2	p_3	p_4	p_5
0	4.730	7.853	10.996	14.137

Ω_1	Ω_2	Ω_3	Ω_4	Ω_5
0	23.373κ	61.671κ	120.91κ	199.57κ

For the fixed-fixed beam:

$$\Xi_i(\xi) = \cos p_i\xi - \cosh p_i\xi + \frac{\sin p_i + \sinh p_i}{\cos p_i - \cosh p_i}(\sin p_i\xi - \sinh p_i\xi)$$

$$\cos p_i \cosh p_i = 1.$$

p_1	p_2	p_3	p_4	p_5
4.730	7.853	10.996	14.137	17.279

Ω_1	Ω_2	Ω_3	Ω_4	Ω_5
23.373κ	61.671κ	120.91κ	199.57κ	298.57κ

For the fixed-free beam:

$$\Xi_i(\xi) = \cos p_i \xi - \cosh p_i \xi + \frac{\sin p_i - \sinh p_i}{\cos p_i + \cosh p_i} (\sin p_i \xi - \sinh p_i \xi)$$

$$\cos p_i \quad \cosh p_i = -1$$

p_1	p_2	p_3	p_4	p_5
1.875	4.694	7.855	10.996	14.137

Ω_1	Ω_2	Ω_3	Ω_4	Ω_5
3.516 K	22.034 K	61.701 K	120.91 K	199.57 K

For the fixed-hinged beam:

$$\Xi_i(\xi) = \cos p_i \xi - \cosh p_i \xi - \frac{\cos p_i + \cosh p_i}{\sin p_i + \sinh p_i} (\sin p_i \xi - \sinh p_i \xi)$$

$$\tan p_i = \tanh p_i$$

p_1	p_2	p_3	p_4	p_5
3.927	7.069	10.210	13.352	16.493

Ω_1	Ω_2	Ω_3	Ω_4	Ω_5
15.421 K	49.971 K	104.25 K	178.27 K	272.02 K

For the free-hinged beam:

$$\Xi_i(\xi) = \cos p_i \xi + \cosh p_i \xi - \frac{\cos p_i + \cosh p_i}{\sin p_i + \sinh p_i} (\sin p_i \xi + \sinh p_i \xi)$$

$$\tan p_i = \tanh p_i$$

p_1	p_2	p_3	p_4	p_5
0	3.927	7.069	10.210	13.352

Ω_1	Ω_2	Ω_3	Ω_4	Ω_5
0	15.421 K	49.971 K	104.25 K	178.27 K

APPENDIX II

As noted on page 10, the functions $\Xi_i(\xi)$ constitute a normalized orthogonal set. It has long been known (15), (17), that these functions are orthogonal. That they are normal is most easily shown by direct evaluation. To this end we recall the identities:

$$\int_0^1 \Xi_i^2 \, d\xi = -\frac{1}{2}\left(\frac{d\Xi_i}{d(p_i\xi)} \cdot \frac{d^3\Xi_i}{d(p_i\xi)^3}\right)\Bigg|_{\xi=1}$$

if the right end of the beam is hinged;

$$\int_0^1 \Xi_i^2 \, d\xi = \frac{1}{4}\left(\Xi_i\right)^2\Big|_{\xi=1}$$

if the right end of the beam is free; and

$$\int_0^1 \Xi_i^2 \, d\xi = \frac{1}{4}\left(\frac{d^2\Xi_i}{d(p_i\xi)^2}\right)^2\Bigg|_{\xi=1}$$

if the right end of the beam is fixed.

Substitution of the appropriate expression for Ξ_i in the above identities and appeal to the identity embodied in the frequency equation leads to the value of 1 for the integral. Thus*

1. <u>For the hinged-hinged beam:</u>

$$\frac{d\Xi}{d(p\xi)} = \sqrt{2}\cos p\xi \qquad\qquad \frac{d^3\Xi}{d(p\xi)} = -\sqrt{2}\cos p\xi$$

---

* Throughout the remainder of this Appendix the subscript i is omitted for economy of writing.

$$\therefore \int_0^1 \Xi_i^2 \, d\xi = -\tfrac{1}{2}(\sqrt{2}\cos p)(-\sqrt{2}\cos p)$$

$= \cos^2 p = 1$ since $\sin p = 0$.

2. For the free-free beam:

$$\int_0^1 \Xi^2 \, d\xi = \tfrac{1}{4}\left[\cos p + \cosh p + \frac{\sin p + \sinh p}{\cos p - \cosh p}(\sin p + \sinh p)\right]^2$$

$$= \frac{1}{4}\left[\frac{\cos^2 p - \cosh^2 p + \sin^2 p + 2\sinh p \sin p + \sinh^2 p}{\cos p - \cosh p}\right]$$

$$= \frac{\sin^2 p \sinh^2 p}{(\cos p - \cosh p)^2}$$

$$= \frac{(1-\cos^2 p)(\cosh^2 p - 1)}{\cos^2 p - 2\cos p \cosh p + \cosh^2 p}$$

$$= \frac{\cosh^2 p - \cos^2 p \cosh^2 p + \cos^2 p - 1}{\cos^2 p - 2 + \cosh^2 p}$$

$= 1$ since $\cos p \cosh p = 1$

3. For the fixed-fixed beam:

$$\frac{d^2 \Xi}{d(p\xi)^2} = -\cos p\xi - \cosh p\xi + \frac{\sin p + \sinh p}{\cos p - \cosh p}(-\sin p\xi - \sinh p\xi)$$

$$\therefore \int_0^1 \Xi^2 \, d\xi = \frac{1}{4}\left[\frac{d^2 \Xi}{d(p\xi)^2}\right]^2_{\xi=1} = 1$$

by comparison with the evaluation for the free-free beam.

4. <u>The fixed-free beam:</u>

5. <u>The fixed-hinged beam:</u>

6. <u>The free-hinged beam:</u>

These demonstrations are carried out in the same manner as the foregoing and will not be shown here.

APPENDIX III

Speed of Sound in Solids at Room Temperatures

Metal	a x 10^{-5} inches/sec.
Aluminum	1.980 - 2.070
Brass	1.265 - 1.423
Copper	1.401 - 1.567
Gold	0.686 - 0.819
Iron	1.933 - 2.018
Magnesium	1.811
Nickel	1.956
Platinum	1.058 - 1.099
Silver	1.042 - 1.054
Steel	1.961 - 2.003
Zinc	1.449 - 1.455

NOTE: a decreased with increasing temperature.

a increases with hardness.

This table compiled from the International Critical Tables, Alcoa Handbook, Trade publications of E. I. du Pont Co., Allegheny Ludlum Steel Corp. and others.

APPENDIX IV

Expansion of the Statical Deflection curve of a Cantilever Beam with a Concentrated Load at the Free End in an Infinite Series of Eigen-functions.

The statical deflection curve for a cantilever beam whose root is at (0,o) and whose free end before deflection is at (ℓ,0) referred to a pair of x-y axes is

$$y = \frac{Px^2}{6EI}(3\ell - x) \tag{91}$$

In dimensionless form this becomes if we write $\theta^2 = \frac{P}{6EA}$

$$\eta = \frac{\theta^2}{k^2}\xi^2(3-\xi) \tag{92}$$

For such a beam the eigen-function expansion (See Appendix I) is

$$\eta = \sum_{i=1}^{\infty} a_i \Xi_i(\xi) \tag{93}$$

where

$$\Xi_i(\xi) = \cos p_i\xi - \cosh p_i\xi + \frac{\sin p_i - \sinh p_i}{\cos p_i + \cosh p_i}(\sin p_i\xi - \sinh p_i\xi) \tag{94}$$

In order to evaluate the a_i, the right-hand side of Eq. (92) is substituted for the left hand-side of Eq. (93). The equation is then multiplied through by $\Xi_i(\xi)$ and the result integrated term-wise from 0 to 1. All terms in the right-hand side save that containing a_i vanish because of the orthogonality of the Ξ_i and the coefficient of the a_i is 1 because of their normality.

Hence

(95) $$a_i = \int_0^1 \frac{\Theta^2}{K^2} \xi^2(3-\xi)\, \Xi_i(\xi)\, d\xi$$

The integration which is easily carried out, though somewhat tedious yields

(96) $$a_i = \frac{12\,\Theta^2}{p_i^4 K^2}$$

The expression for the statical deflection of the beam is then

(97) $$\eta = \frac{\Theta^2}{K^2} \xi^2(3-\xi) = \sum_{i=1}^{\infty} \frac{12\,\Theta^2}{p_i^4 K^2} \Xi_i(\xi)$$

In order to compare the stress at the root of the beam when it is vibrating in its first mode only with the corresponding statical stress it is only to compare the second derivatives of the third and second members, resp., of Eq. (97) for i = 1. This yields

(98) $$\frac{d^2}{d\xi^2}\left[\frac{12\,\Theta^2}{p_i^4 K^2} \Xi(\xi)\right]_{\xi=0} = \frac{24\,\Theta^2}{p_i^2 K^2}$$

and

(99) $$\frac{d^2}{d\xi^2}\left[\frac{\Theta^2}{K^2} \xi^2(3-\xi)\right]_{\xi=0} = \frac{6\,\Theta^2}{K^2}$$

The ratio, R, of the stresses under consideration is

(100) $$R = \frac{4}{p_i^2} = 1.137 \qquad \text{since} \quad p_1 = 1.875$$

Hence, an over-stress of as much as 114 percent of the statical stress can be anticipated at the root of the beam if the load is suddenly removed.

APPENDIX V.

The Frequency Equation for Frames.

In Eq. (38), if we postulate vibration in symmetrical modes, the last term will vanish. The differential equations of motion are

(101) $$EI_1 \frac{\partial^4 y}{\partial x^4} + \frac{A_1 \gamma}{g} \frac{\partial^2 y}{\partial t^2} = 0$$

(102) $$EI_2 \frac{\partial^4 v}{\partial u^4} + \frac{A_2 \gamma}{g} \frac{\partial^2 v}{\partial t^2} = 0$$

The boundary conditions to be satisfied are:

(103) At A: $$\delta y\Big|_{x=0} = 0 \quad \text{and} \quad \frac{\partial^2 y}{\partial x^2}\Big|_{x=0} = 0.$$

(104) At B: $$\delta y\Big|_{x=l_1} = 0 \quad \text{and} \quad \delta v\Big|_{u=0} = 0.$$

Because of symmetry:

(105). $$\delta \frac{\partial v}{\partial u}\Big|_{u=0} = -\delta \frac{\partial v}{\partial u}\Big|_{u=l_2}$$

(106) $$\frac{\partial^2 v}{\partial u^2}\Big|_{u=0} = \frac{\partial^2 v}{\partial u^2}\Big|_{u=l_2}$$

hence $$\left(\frac{\partial^2 v}{\partial u^2} \delta \frac{\partial v}{\partial u} - \frac{\partial^3 v}{\partial u^3} \delta v\right)\Big|_0^{l_2} = 2 \frac{\partial^2 v}{\partial u^2} \delta \frac{\partial v}{\partial u}\Big|_{u=0} \quad \text{and}$$

(107) $$2EI_1 \frac{\partial^2 y}{\partial x^2} \delta \frac{\partial y}{\partial x}\Big|_{x=l_1} + 2EI_2 \frac{\partial^2 v}{\partial u^2} \delta \frac{\partial v}{\partial u}\Big|_{u=0} \text{ must } = 0.$$

Because of the rigidity of the joints

(108) $$\frac{\partial y}{\partial x}\Big|_{x=l_1} = \frac{\partial v}{\partial u}\Big|_{u=0}$$

and

(109) $$EI_1 \frac{\partial^2 y}{\partial x^2}\Big|_{x=l_1} = EI_2 \frac{\partial^2 v}{\partial u^2}\Big|_{u=0}$$

so that Eq. (107) is satisfied. The variation equation, Eq. (88), is then satisfied and Eqs. (108) - (109) are the boundary conditions.

We can proceed in the usual fashion and assume that y can be expressed as

(110) $$y = X(x)\,T(t)$$

while v can be expressed as

(111) $$v = U(u)\,T(t)$$

The T(t) will be the same function in both expressions. Upon separating variables we have

(112) $$T = A \cos pt + B \sin pt$$

(113) $$X = a_1 \sin k_1 x + b_1 \cos k_1 x + c_1 \sinh k_1 x + d_1 \cosh k_1 x$$

and

(114) $$U = a_2 \sin k_2 u + b_2 \cos k_2 u + c_2 \sinh k_2 u + d_2 \cosh k_2 u$$

where

(115) $$k_1 = \frac{A_1 \gamma p^2}{EI_1 g} \qquad \text{and} \qquad k_2 = \frac{A_2 \gamma p^2}{EI_2 g}$$

Upon substituting Eqs. (113) and (114) in the boundary conditions we find the frequency equation in the form

(116) $$\cos \frac{k_2 l_2}{2} \left\{ \frac{\alpha}{2\beta} \left(\cot \frac{k_2 l_2}{2} + \coth \frac{k_2 l_2}{2}\right)\left(\cot k_1 l_1 - \coth k_1 l_1\right) + 1 \right\} = 0$$

where $\frac{\alpha}{2\beta}$ has been written for $\frac{I_2}{2I_1}\sqrt[4]{\frac{A_2 I_1}{A_1 I_2}}$. The roots of the first factor are easily enough obtained. To obtain the roots of the second factor we let $\frac{l_2}{2}\sqrt[4]{\frac{A_2\gamma}{EI_2 g}}$ = a and $l_1\sqrt[4]{\frac{A_1\gamma}{EI_1 g}}$ =b. The factor assumes the form

$$(117) \qquad \cot a\sqrt{p} + \coth a\sqrt{p} = \frac{-c}{\cot b\sqrt{p} - \coth b\sqrt{p}} \; ; \quad \text{where} \quad c = \frac{2\beta}{\alpha}$$

which is readily solved numerically in any given case. Once the frequency equation has been solved, the deflections, stresses, etc., at any point of the structure are obtained from Eqs. (110) - (115) in the ordinary way.